Methyl jasmonate treatment affects the regulation of the 2-C-methyl-D-erythritol 4-phosphate pathway and early steps of the triterpenoid biosynthesis in *Chlamydomonas reinhardtii*

Audrey S. Commault[1], Michele Fabris[1,2], Unnikrishnan Kuzhiumparambil[1], Jack Adriaans[1], Mathieu Pernice[1] and Peter J. Ralph[1].*

[1]University of Technology Sydney, Climate Change Cluster, Ultimo NSW 2007, Australia

[2]CSIRO, Synthetic Biology Future Science Platform, Brisbane QLD 4001, Australia.

*Corresponding author at: University of Technology Sydney, Climate Change Cluster, Ultimo NSW 2007, Australia.

Email: audrey.commault@uts.edu.au

Highlights

- First report of triterpenoid elicitation by a phytohormone in *C. reinhardtii*
- MeJA treatment (1 mM) arrested the growth and up-regulated genes of the MEP pathway
- Highlighting a specialised pathway branching immediately upstream of cycloartenol
- Accumulation of an uncharacterised triterpenoid secondary metabolite ($C_{30}H_{52}O_3$)
- Plant-like MeJA response machinery is putatively absent in *C. reinhardtii*

ABSTRACT

Terpenoids are a large and diverse class of naturally occurring metabolites serving many industrial applications and natural roles. Economically important terpenoids are often produced in low abundance from their natural sources, making their industrial-scale production challenging or uneconomical, therefore engineered microorganisms are frequently used as heterologous production platforms. Photosynthetic microorganisms, such as the green alga *Chlamydomonas reinhardtii*, represent promising systems to produce terpenoids in a cost-effective and sustainable manner, but knowledge about the regulation of their terpenoid metabolism remains limited. Here we report on the investigation of the phytohormone methyl jasmonate (MeJA) as elicitor of algal terpenoid synthesis. We treated *C. reinhardtii* cells in mid-exponential growth phase with three different concentrations of MeJA (0.05, 0.5 and 1 mM). The highest concentration of MeJA affected the photosynthetic activity of the cells, arrested the growth and up-regulated key genes of the 2-C-methyl-D-erythritol 4-phosphate (MEP) pathway, leading to a significant increase in intermediates of this pathway, squalene and (*S*)-2,3-epoxysqualene, while the abundance of cycloartenol, and two main sterols (ergosterol and 7-dehydroporiferasterol) decreased. These data suggest the redirection of the carbon flux towards the synthesis of yet uncharacterised triterpenoid secondary metabolites upon MeJA treatment. Our results offer important new insights into the regulation of the triterpenoid metabolism in *C. reinhardtii* and raise important questions on hormonal signalling in microalgae. Phytohormone treatment is tested for the first time in algae, where it holds great potential for identifying key transcriptional regulators of the MEP pathway as targets for future metabolic engineering studies for improve production of high-value triterpenoids.

Keywords: microalgae; methyl jasmonate; methyl-D-erythritol 4-phosphate (MEP) pathway; *Chlamydomonas reinhardtii*; triterpenoids; sterols.

1. INTRODUCTION

Terpenoids (isoprenoids) are the largest class of natural compounds, which are involved in a myriad of cellular processes. Their diverse biological activities have found applications in multiple industrial products (pharmaceutics, nutraceutics, agriculture, chemicals, flavours/fragrances, colourants, fuels/fuel additives) [1, 2]. Most commercially relevant terpenoids known today are isolated from higher plants, but their industrial production is often challenging or uneconomical, as they are produced in low abundance and only under specific conditions. Thus, their production and extraction from plants requires large amounts of biomass, the yields can vary significantly from batch to batch and the extraction/purification processes are labour intensive and expensive [2-4]. Further, the chemical synthesis of these compounds, when possible, is often too costly and complex, as correct chirality is usually required [1]. In light of these challenges, bioengineering of microbes for the production of terpenoids in controlled bioreactors has emerged as a viable solution. The model organisms *Saccharomyces cerevisiae* (yeast) and *Escherichia coli* (bacteria) are typically chosen as heterologous hosts for terpenoid production due to the relative ease of cultivation, the detailed knowledge of their metabolism and their genetic tractability [1]. The use of these organisms, however, is driven by their well-developed genetic toolbox rather than their terpenoid metabolism [5], as both yeast and bacteria do not naturally synthesise plant metabolites. Moreover, both organisms rely on organic carbon sources for growth; consequently adding cost to the production of industrially relevant terpenoids. In recent years, engineered

photosynthetic microbial hosts have emerged as a carbon-neutral alternative to commonly used fermentative systems, as they have the ability to convert inorganic carbon (CO_2) into useful biochemicals [6]. Proof-of-principle heterologous terpenoid expression have been reported for cyanobacteria, the diatom *Phaeodactylum tricornutum* and the model eukaryotic green microalga *Chlamydomonas reinhardtii* [7-10]; however, as of today, these organisms are less tractable and often produce lower yields than engineered *E. coli* and yeast.

The universal terpenoid precursors isopentenyl diphosphate (IPP) and dimethylallyl diphosphate (DMAPP) are naturally produced via two independently evolved isoprenoid pathways: the mevalonate (MVA) pathway and the methyl-D-erythritol 4-phosphate (MEP) pathway, of which *C. reinhardtii* only possesses the latter [11]. IPP and DMAPP are then condensed to geranyl diphosphate (GPP), farnesyl diphosphate (FPP) and geranylgeranyl diphosphate (GGPP), which are the 'building blocks' of specialised terpenoids (Figure 1). The heterologous synthesis of terpenoids generally consists in the expression of enzymes or even entire biosynthetic pathways, which connect to endogenous terpenoid metabolism and convert the prenyl phosphate substrates into the desired product [9, 12, 13]. Engineering of upstream terpenoid pathways (MVA and/or MEP) is usually necessary to obtain higher yields [1, 12]. In *C. reinhardtii*, IPP and DMAPP must be generated entirely from the MEP pathway in the chloroplast (Figure 1). For sustainable and cost-effective production of terpenoids in microalgae, metabolic engineering of the MEP pathway is necessary to increase the flow of carbon towards the production of terpenoids precursors [7, 11]. However, very little is known about the MEP pathway regulation and the mechanisms of IPP and DMAPP transport in *C. reinhardtii*. A number of promising strategies have been suggested for MEP pathway deregulation in photosynthetic microorganisms, such as the inhibition of competing metabolic pathways, gene over-expression, screening of enzyme variants with increased activity, enzyme fusions and inhibition of post-translational events [7, 14]. In this study, we

investigated a plant hormone, methyl jasmonate (MeJA), as a potential elicitor of the MEP pathway in *C. reinhardtii*. Plants produce MeJA as a signalling compound in response to biotic and abiotic stresses (e.g., pathogen attack, herbivory and wounding), triggering a complex signalling cascade that rapidly reprograms cell metabolism and physiology for defence [15, 16]. MeJA is a well-known elicitor of secondary metabolism in plant tissues and exogenous treatment with this hormone has been shown to trigger the biosynthesis of all three major classes of secondary metabolites (i.e. terpenoids, phenylpropanoids/flavonoids, and alkaloids) involved in development and defence mechanisms [3, 17-21]. In higher plants, MeJA is known to upregulate the MEP pathway [22, 23] and has been used as an elicitor to increase the production of high-value terpenoids, such as the synthesis of the anti-cancer agent paclitaxel (Taxol®) in suspension cultures of *Taxus* cell [24].

Although naturally occurring jasmonate signalling has never been reported in microalgae, one study has examined the effect of MeJA on the primary metabolism of *C. reinhardtii* cells, showing a profound perturbation of the central carbon flux and saturated fatty acid metabolism [25]; however, the effect of MeJA on the production of terpenoids by *C. reinhardtii* remains unexplored. Here, we thoroughly investigated the effects of the plant hormone on the production of triterpenoids and isoprenoids precursors in *C. reinhardtii*. This study is one of the first attempts aiming to elucidate the regulation of terpenoid metabolism in *C. reinhardtii*. It sets the basis of future metabolic engineering works for the heterologous production of terpenoids in algae. In the long-term, the knowledge generated will contribute towards the sustainable production of terpenoids in microalgae.

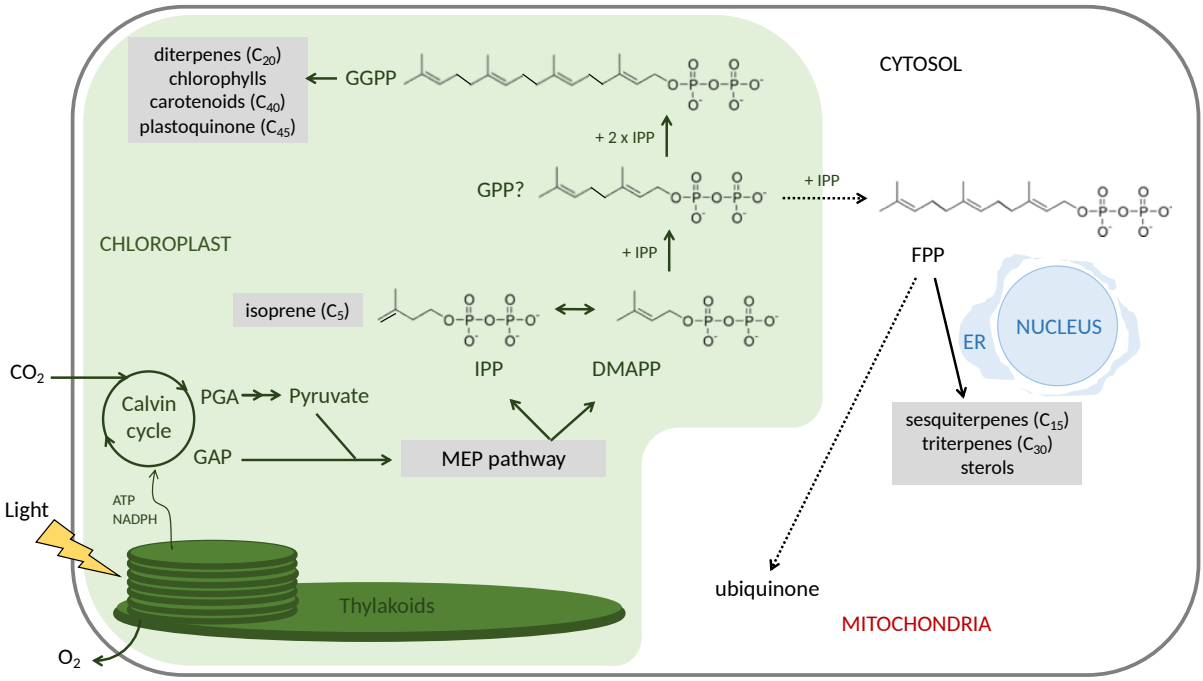

Figure 1. Overview of terpenoid biosynthesis in *C. reinhardtii*. The enzymes of the methylerythritol 4-phosphate (MEP) pathway are nucleus-encoded and post-translationally imported into the chloroplast [11]. The FPP synthase of *C. reinhardtii* is associated with the endoplasmic reticulum [9]. GPP was not detected in this study, therefore a question mark is included. The nature of the transporter(s) responsible for the transfer of prenyl diphosphates accross the plastid membrane is unknown. ER, endoplasmic reticulum; GAP, glyceraldehyde 3-phosphate; PGA, 3-phosphoglyceric acid; DMAPP, dimethylallyl diphosphate; IPP, isopentenyl diphosphate; MEP, methylerythritol 4-phosphate; FPP, farnesyl diphosphate; GGPP, geranylgeranyl diphosphate; GPP, geranyl diphosphate. Adapted from [9, 12].

2. MATERIALS AND METHODS

2.1. Strains and culture conditions

The *Chlamydomonas reinhardtii* wild-type strain CC-125 mt^+ [137c] was cultivated under mixotrophic conditions in Tris-acetate-phosphate (TAP) medium [26] at 26°C under continuous illumination using cool white fluorescent lights (50 ± 10 µmol photon m^{-2} s^{-1}) with

constant agitation at 110 rpm. The cultures were started at a cell density of 10^5 cells mL^{-1} in 1L baffled Erlenmeyer flasks.

2.2. Bioinformatics analysis

In order to mine for plant-like MeJA response machinery in *C. reinhardtii*, translated sequences of the *Arabidopsis thaliana* genes coronatine-insensitive-1 (*COI1, AT2G39940.1*), the transcription factor *MYC2* (*AT1G32640*), members of the *Jasmonate Zim domain family* (*JAZ1*, *AT1G19180.1*), *JAZ2* (*At1g74950*), *JAZ3* (*AT3G17860*), *JAZ6* (*AT1G72450*), *JAZ9* (*AT1G70700*) and *JAZ10* (*AT5G13220*) were used as query for BLASTp searches conducted on the *Chlamydomonas reinhardtii* v5.5 proteome in the Phytozome database (https://phytozome.jgi.doe.gov), where the latest (v5.6) gene models are housed, using standard settings, on the 20/12/2018, and for iterative search through Jackhmmr (https://www.ebi.ac.uk/Tools/hmmer/search/jackhmmer) with the standard settings using Hidden Markov Models of each query protein family (Supplementary Material).

2.3. Methyl jasmonate treatments

The effect of methyl jasmonate (MeJA) on *C. reinhardtii* was assessed by treating mid-log phase cultures (cell density of 5 x 10^5 – 1 x10^6 cells mL^{-1}) with three different final concentrations of MeJA (0.05, 0.5 and 1 mM). The stock solutions of MeJA were diluted in pure ethanol and prepared so the cultures were all injected with 1% (v/v) ethanol, including the controls. Three biological replicates were used per treatment.

2.4. Automated cell counts

Samples (0.5 mL) were extracted from the flasks at 0, 12 and 48 hours, fixed with 0.2 µm filtered glutaraldehyde at a final concentration of 2% and stored at 4 °C in the dark. A 10 µL aliquot was pipetted into a haemocytometer (Neubauer, Germany) and viewed under a Nikon Eclipse compound microscope (Nikon, Japan) at 10 x magnification. Cells were allowed to settle into the focal plane for 5 min before 12 images of haemocytometer squares were recorded (Nikon DS-Qi2). Images were processed on ImageJ software (version 2.0) using a custom script to calculate number of cells mL^{-1}.

2.5. Chlorophyll *a* fluorescence measurement

Pulse-amplitude modulated fluorometry (PAM) was used to measure the maximum quantum yield of photosystem II (Fv/Fm calculated as Fv = Fm – Fo, where Fo is the minimum fluorescence in the dark and Fm the maximum fluorescence) for rapid assessment of *C. reinhardtii* photosynthetic activity during the experiment, and to monitor for any photosystem stress caused by MeJA treatment. The measurements were taken with a POCKET-PAM (Gademann Instruments GmbH, Germany) after 10 min of dark acclimation. These measurements were performed at room temperature with the following settings: blue light, measuring light intensity <0.2 mmol photons m^{-2} s^{-1} PAR, saturation pulse intensity of 2,700 µmol photons m^{-2} s^{-1} PAR, and saturation pulse width of 0.6 s.

2.6. Metabolites extraction and quantification

2.6.1. Triterpenoid analysis

For triterpenoid analysis, 20 mL of algal culture were harvested at 48 hours after treatment. The cells were pelleted at 4,000 x g for 5 min at 4°C, rinsed once with phosphate buffered saline (PBS) 1x and frozen at -80°C. Cells were freeze-dried and the dry weight was

measured before extracting the metabolites. Extraction and gas chromatography–mass spectrometry (GC–MS) analyses were performed as described in [27].

2.6.2. Isoprenoid analysis

For the analysis of 2-C-methyl-D-erythritol 4-phosphate (MEP), 2-C-methyl-D-erythritol-2,4-cyclodiphosphate (MEcPP), geranyl diphosphate (GPP), geranylgeranyl pyrophosphate (GGPP) and farnesyl pyrophosphate (FPP), 40 mL of algal suspension were washed with 160 mL and 50 mL of cold PBS, respectively and extracted as described by Canelas et al. [28] using PBS instead of methanol and by keeping the samples at -2˚C instead of -40˚C. Ten µM of Azidothymidine (AZT) was used as internal standard. MEP, MEcPP, GPP, GGPP and FPP were analysed using a previously described LC-MS/MS method with slight modifications [29]. Authentic standards were kindly provided by A/Prof Claudia Vickers (University of Queensland, Australia). Samples were analysed in multiple reaction monitoring mode on a mass spectrometer (Agilent 6490 Triple Quadrupole) with ESI source (negative ion mode). Following transitions were monitored with fragmentor voltage of 380 V. MEP (m/z 520 → 322, 520 → 97, 520→ 79, collision energy (CE) -18 eV), MEcPP (m/z 277 → 179, 277 → 97, 277 → 79, CE -15eV), GGPP (m/z 449 → 431, 449 →159, 449 → 79, CE -18eV) and FPP (m/z 381 → 363, 381 → 159, 381 → 79 CE -15eV). Chromatographic separation was performed on an Agilent 1290 LC system with a Phenomenex C-6 phenyl analytical column (250 mm × 4.6 mm, 5 µm). The mobile phase, consisted of 20 mmol/L ammonium hydrogencarbonate solution (A) and Water/Acetonitrile (1:9, v/v) (B), pumped at a flow rate of 1 mL/min. LC separation was performed using a linear gradient program as follows: 5 % B until 1 min, ramped to 100 % B at 10 min, held until 12 min, ramped down to 5 % B at 6 min and held until 18 min. Quantification was performed using the five point calibration curve

plotted using analytical standards. The concentrations were normalized to the internal standard (AZT) and a total of 10^8 cells.

2.6.3. Pigments analysis

Extraction of carotenoids (including chlorophyll a, chlorophyll b and β-carotene) was carried out using 1.5 mL of chilled HPLC-grade acetone and kept in the dark prior to pigment analysis by HPLC-UV. Samples were vortexed for 30 seconds (x 3 times) and stored at -20°C overnight. Pigment extracts were then filtered through 0.2 μm PTFE 13 mm syringe filters and stored at -80°C until analysis. An Agilent 1290 Infinity LC HPLC System equipped with a binary pump with integrated vacuum degasser, thermostatic column compartment modules, an Agilent 1290 Infinity Autosampler and PDA (photo-diode array) detector was used for analysis. A Zorbax Eclipse XDB C8 HPLC 4.6 mm × 150 mm and guard column (Agilent) was used by eluting a gradient of tetrabutyl alkylammonium acetate (TBAA) methanol mix (30:70) (Solvent A) and methanol (Solvent B) as follows: 0–22 min, from 5 to 95% B; 22–29 min, 95% B; 29–31 min, 5% B; 31-40 min, column equilibration with 5% B. Column temperature was maintained at 55°C. A complete pigment spectrum (270 to 700 nm) was recorded using the PDA detector. Response factor measurement was performed using pigment standards obtained from DHI, Denmark.

2.6.4. $C_{30}H_{52}O_3$ and protopanaxadiol profiling

Chemical profile of MeJa treated and control *C. reinhardtii* cells and protopanaxadiol standard (10μg/mL in MeOH) were analysed using 6550 iFunnel Q-TOF LC-MS (Agilent Technologies, Santa Clara, CA, USA) equipped with Dual AJS ESI, coupled with an 1260 infinity HPLC system (Agilent Technologies, Santa Clara, CA, USA). Separation was performed at 25°C on an Agilent Zorbax Eclipse XDB-C18 column (150 × 4.6 mm i.d., 2.7

μm). The HPLC program consisted of a linear gradient of A (milli-Q water with 1 % formic acid) to B (100% acetonitrile with 1% formic acid) over 25 min, followed by isocratic elution at B at a flow rate of 1 mL min^{-1}. Nitrogen was used as the nebulizing gas. Dual Automatic Jet Stream (AJS) Electrospray Ionisation (ESI) source was kept at a voltage of 3500 V in positive ion mode. Mass spectra were acquired with source conditions as follows: gas temperature 350°C, drying gas 4 L min^{-1} (N_2), nebulizer pressure 35 psi (N_2) and Vcap 3,500 V, fragmentor 160V and skimmer 65 V. The mass range scanned was 70–1100 m/z.

2.7. Gene expression (qPCR)

The present study conforms to the Minimum Information for Publication of Quantitative Real-Time PCR guidelines [30]. In this section, we indicate the essential information, sensu Bustin et al. (2009), required to allow reliable interpretation of the corresponding RT-qPCR results.

2.7.1. Primer design

The transcript sequences coding for the enzymes of the methylerythritol phosphate (MEP) pathway, the FPP synthase (FPPS), the cycloartenol synthase (CAS), the squalene monooxygenase, the sterol C-14 demethylase (CYP51), and delta14-sterol reductase (EGR4/24) were obtained from the Phytozome *Chlamydomonas reinhardtii* v5.5 database (https://phytozome.jgi.doe.gov). The transcript sequences were blasted for functional domains (Blastx, https://blast.ncbi.nlm.nih.gov/Blast.cgi), which were used as template to design sequence-specific primers for RT-qPCR using the software Primer3 version 4.1.0 (http://bioinfo.ut.ee/primer3/; Table 1) [31].

Table 1. Sequence-specific primers used in this study for RT-qPCR analysis. Target name, *C. reinhardtii* gene IDs, primers sequences, amplicons length, melting temperatures, and RT-qPCR efficiencies are indicated. DXS: 1-deoxy-D-xylulose 5-phosphate synthase; DXR: 1-deoxy-D-xylulose 5-phosphate reductoisomerase; CMK: 4-(cytidine 5'-diphospho)-2-C-methyl-D-erythritol kinase; MDS: 2-C-methyl-D-erythritol 2,4-cyclodiphosphate synthase; IDI: Isopentenyl-diphosphate Delta-isomerase; FPPS: Farnesyl pyrophosphate synthase; SQE: Squalene epoxidase; CAS: Cycloartenol synthase; CYP51: sterol C-14 demethylase; ERG4/24: delta14-sterol reductase; CBLP: *Chlamydomonas* β subunit-like polypeptide; RPL13: ribosomal protein L13; RPL10a: ribosomal protein L10a.

Name	Gene ID/Reference	Enzymatic function ‡	Primer forward sequence	Primer reverse sequence	Length (bp)	Tm (°C)	Efficiency (%)
DXS	Cre07.g356350.t1.1	Putative	ACGTTGTCCAGAAGGCAACT	GATGAGGTCGTCCAGGTTGT	137	59.8	99.9
DXR	Cre12.g546050.t1.2	Putative	GAGTTCCCCGACAAGTTCAA	ATCCTTCACAGCCACCATCT	108	59.5	95.1
CMK	Cre02.g145050.t1.2	Putative	GAAGCCTCAGCAGGATTACG	GACCGCCTCTTCCAACATAA	102	60.0	98.0
MDS	Cre12.g503550.t1.2	Putative	GAGAACATCCGCAACAACCT	CAGGCTATCCACCTTCTCGT	93	59.3	100.0
IDI †	Cre08.g381800.t1.1	Putative	GGTGACGCTGACACAGGAG	CGTTGTCCTGAATCCCTTGT	101	60.0	98.9
FPPS	Cre03.g207700.t1.1	Putative	GGGCCAGTACTTTCAGATCC	ACTTGTTGTCCTCGATGTCC	95	60.1	101.3
SQE	Cre17.g734644.t1.1	Validated §	CAGACGGCGGACTTTTACAC	CCTTCAGGAATACGGTACGC	119	59.6	100.5
CAS	Cre01.g011100.t1.2	Putative	CATCCTGAGCTACCAGAACC	GCTGTAGTCCACGATGATGT	121	59.9	96.1
CYP51	Cre02.g092350.t1.2	Putative	TTGATGTGGAGCAGAAGGTC	GAAATCAACAACGCCCGTC	149	60.0	94
ERG4/24	Cre02.g076800.t1.2	Putative	CTTGCATGGTTTTTCGGTGT	AAGGCGTTCAGCTTGTATGT	110	60.0	79.5
CBLP	Zhao et al., [32]	-	TGCTGTGGGACCTGGCTGA	GCCTTCTTGCTGGTGATGTTG	193	61.5	100.8
RPL13	Whitney et al., [33]	-	AGCACGGCTAGAGACAGATG	TAGTGCGTGGCTGTTTGTTG	115	57.0	100.0
RPL10a	Pape et al. [34]	-	CCAAGTGCAGCATCAAGTTC	CACGTTCTGCCAGTTCTTCT	152	56.0	89.5

† IDI is predicted to be present in two different isoforms in *C. reinhardtii*. The absence of amplification for the second isoform (Cre11.g467544.t1.1) lead us to focus only on one isoform.

‡ Enzymatic function: Validated = experimental evidence at protein level and/or experimental evidence at transcript level; Putative = protein function inferred by homology and/or protein predicted

§ [35]

2.7.2. RNA extraction and cDNA synthesis

For gene expression analysis, 50 mL aliquots were extracted from the culture flasks at 48 hours. *C. reinhardtii* cells were pelleted at 4,000 x g for 5 min at 4°C, rinsed once with PBS 1x and flash frozen in liquid nitrogen. Frozen pellets were stored at -80 °C until RNA extraction. The RNA was extracted by adding 1.5 mL of PureZol (Bio-Rad) to the frozen pellet and pipetting up and down 5 times to homogenize. After 5 min incubation at room temperature, 300 µL of chloroform was added. The sample was gently mixed for 15 seconds and incubated at room temperature for 15 min before being centrifuged at 12,000 x g for 15 min at 4 °C. The upper phase was recovered and mixed with an equal volume of absolute ethanol. The sample was then transferred to an RNeasy mini spin column provided with the RNeasy Mini Kit (Qiagen) and the rest of the extraction was performed according to manufacturer's instructions. Column purification was carried out to remove gDNA using PureLink™ DNase (Life Technologies). The RNA quantity was assessed by spectrophotometry (NanoDrop™, 2000, Thermo Scientific). The quantity of RNA was normalized to 1 µg in all the samples, for accurate comparison between treatments, and used for further cDNA synthesis. The cDNA was generated using an iScript cDNA Synthesis Kit (Bio-Rad) following the manufacturer's instructions and stored at -20 °C.

2.7.3. RT-qPCR

RT-qPCR gene expression quantification was performed in three technical replicates using iTaq UniverSYBR Green Master Mix (Bio-Rad) on a Real-Time PCR System (CFX384™, Bio-Rad). A total volume of 10 µL per reaction was used with 1:20 dilutions of cDNA from control and treated *C. reinhardtii* cells and 100 nM of each specific primers (final concentration). The Hard-Shell® 384-Well PCR plates (Bio-Rad) were filled with a robot (epMotion 5075, Eppendorf) and the amplification was performed using the following PCR

conditions: incubation at 95 °C for 10 min, then 44 cycles of 95 °C, 60 °C, 68 °C for 30 s each, followed by a melt curve. A "no template" control along with a "no reverse transcription" control were generated for each gene and each treatment to ensure that the PCR reactions were free of genomic DNA contamination. Repeatability of the assay between the technical replicates was consistent across the different genes with the replicate variability falling within the set limit of <0.5 cycles for all the sample-gene combinations tested.

2.7.4. Data acquisition

The RT-qPCR data were analysed in regression mode using the CFX Manager™ 3.1 Software. The RT-qPCR efficiency for each gene and each treatment was determined against a standard curve (cDNA dilution gradient of 243, 81, 27, 9 and 3 ng) and a linear regression model [36]. The corresponding RT-qPCR efficiencies were calculated according to the equation described by Radonić et al. [37]:

$$PCR\ efficiency\ = \left(10^{\left[-\frac{1}{slope}\right]} - 1\right) \times\ 100$$

All of the RT-qPCR efficiencies obtained for the different primers were between 80 and 101% (Table 1), with a calibration coefficient >0.95 as previously recommended [30]. Expression levels of the target genes were normalized against the three reference genes (CBLP, RPL13, RPL10a; Table 1) to obtain Normalized Relative Quantities (NRQ).

2.8. Statistical analyses

Statistical analyses were done in GraphPad Prism 5.0 Kolmogorov-Smirnov and Levene'test were used first to confirm normality and homoscedasticity of the data respectively, and parametric tests (ANOVA and unpaired *t*-test) were applied accordingly. Significant effects were then analysed using post-hoc Tukey's HSD test for the cell count and Fv/Fm data, a

Dunnett's test for the RT-qPCR data and a two-tailed unpaired *t*-test for the metabolite concentrations. The analyses tested the null hypothesis that there was no difference in growth, chlorophyll *a* fluorescence, gene expression and metabolites abundance between the MeJA-elicited and control treatments. The results were considered significant at $P < 0.05$ (Table A1). Throughout the paper, values given are mean ± SEM (n = 3 biological replicates).

3. RESULTS AND DISCUSSION

3.1. Potential absence of a plant-like MeJA response machinery in *C. reinhardtii*

Higher plants respond to methyl jasmonate (MeJA) through a complex signalling cascade that triggers profound transcriptional, translational and metabolic reprogramming of cell physiology. In *A. thaliana* the upstream players and regulators of this mechanism include coronatine- insensitive-1 (COI1) factor, cullin-1 (CUL1), the transcriptional regulator MYC2 and members of the Jasmonate Zim domain (JAZ) protein family [38, 39]. The proteome of *C. reinhardtii* was mined for orthologs or proteins related to COI1, CUL1, MYC2 and JAZ proteins, but no significant matches to the query proteins could be identified, with the exception of a homolog of CUL1 (Cre17.g734400.t1.1). *C. reinhardtii* possesses at least three members of the Cullin protein family (Cre17.g734400.t1.1, Cre07.g324050.t1.2 and Cre12.g516500.t1.1), which are knowingly involved in protein degradation mechanisms, and widely conserved in eukaryotes [40]. Although it cannot be excluded that a plant-like mechanism of MeJA response involving Cre17.g734400.t1 may exist in *C. reinhardtii*, the lack of homologues of key components such as COI1, MYC2 and JAZ proteins, based on our computational analysis, suggests that the mechanism might be different. However, when *C.*

reinhardtii cultures are experimentally treated with sufficient concentration of MeJA, the alga showed a marked physiological and metabolic shift, similar to those generally observed in higher plants [25]. This may suggest the existence of a possibly distinct but convergent MeJA reception and signal transduction mechanism in green algae.

3.2. Effect of MeJA on cell growth and photosynthetic activity

The treatment of *C. reinhardtii* cells with 1 mM of MeJA arrested the growth (two-way ANOVA: $F_{6, 16} = 7.161$, $p = 0.0008$; post-hoc Tukey's HSD $p < 0.0001$; Table A1) and significantly reduced the photosynthetic activity of the cells (two-way ANOVA: $F_{6, 16} = 5.623$, $p = 0.0026$; post-hoc Tukey's HSD $p < 0.01$; Table A1). Lower concentrations of MeJA did not show significant effect (Figure 2). After 48 hours of incubation with 1 mM of MeJA the growth was halted but no signs of apoptosis or cell lysis were observed (Figure A1). A study by Lee et al. [25] reported similar results, with a full inhibition of *C. reinhardtii* growth after treatment with 1 mM of MeJA, while only a partial inhibition was observed at a concentration of 0.5 mM. Lee et al. study also indicated that MeJA-mediated growth inhibition was associated with perturbations in central carbon and saturated fatty acid metabolisms of *C. reinhardtii*. In higher plants, MeJA has been shown to broadly divert carbon allocation from primary metabolism to secondary metabolism [18], which is often accompanied by a decrease in cell growth [24, 41]. The inhibitory effect of MeJA on plant growth is not attributable to cell death, but rather to perturbations of the cell cycle progression [15, 24, 42].

The maximum quantum yield of photosystem II (PSII) dropped from 0.84 ± 0.04 to 0.67 ± 0.07 after 12 hours and 48 hours of incubation with 1 mM of MeJA, respectively

(Figure 2B). In plants, genes involved in photosynthesis, such as ribulose bisphosphate carboxylase/oxygenase, chlorophyll a/b-binding protein, and light-harvesting complex II have been shown to be downregulated following MeJA treatment [16]. Reduced chlorophyll *a* content have been reported in plants [43, 44] as well as the marine red macroalga *Gracilaria dura* [45] when exposed to MeJA. In *C. reinhardtii*, a lower photosynthetic activity is likely to negatively impact cell growth as the cell is impaired in its capacity to generate energy from light. This could partly explain the lower cell density observed 48 hours after MeJA treatment (1 mM).

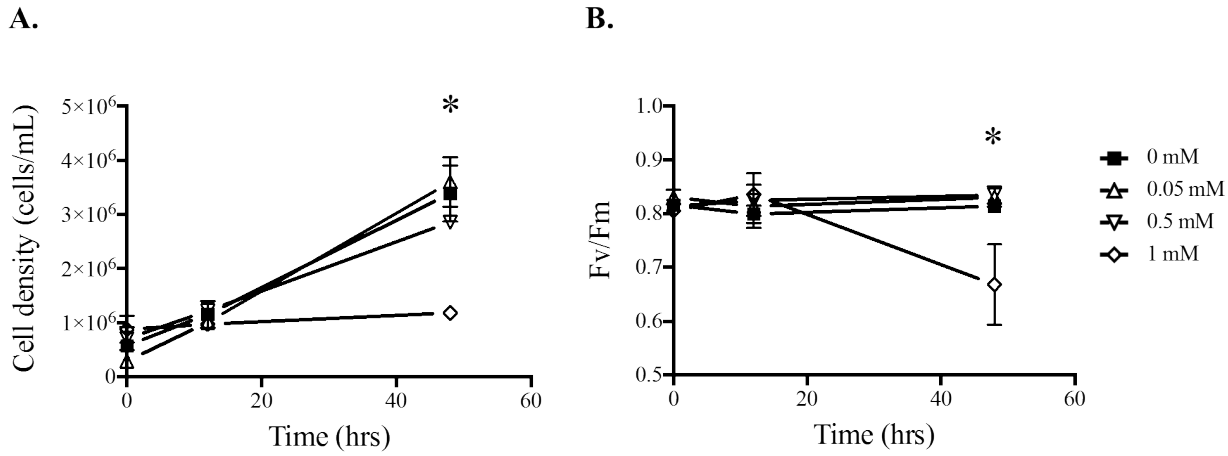

Figure 2. Effect of MeJA concentrations (0, 0.05, 0.5 and 1 mM) on the growth (A) and photosynthetic activity (B) of *C. reinhardtii* cells. The initial 0 hour represents the time at which the cells were treated with MeJA. *Significant difference (post-hoc Tukey's HSD, $P<0.05$) between the control (0 mM) and the 1 mM treatment. Mean ± SEM is shown (n = 3).

3.3. Transcriptional up-regulation of the MEP pathway in MeJA-elicited microalgae

Given the elicitory effect of MeJA on terpenoid production in higher plants, we hypothesized that MeJA induces the biosynthesis of terpenoid precursors in *C. reinhardtii* cells. Isopentenyl

pyrophosphate (IPP) and dimethylallyl pyrophosphate (DMAPP) are the universal building blocks of all terpenoids. In the absence of the mevalonate (MVA) pathway, these precursors are solely synthesized by the methyl-D-erythritol 4-phosphate (MEP) pathway in *C. reinhardtii* [46]. Therefore, the expression levels of five key genes of the MEP pathway were investigated after exposure to MeJA (Figure 3A). Due to significant effects observed on growth and quantum yield of PSII, gene expression data were collected at 48 hours of MeJA treatment. These genes encode the enzymes 1-deoxy-D-xylulose 5-phosphate synthase (DXS, Cre07.g356350.t1.1), 1-deoxy-D-xylulose 5-phosphate reductoisomerase (DXR, Cre12.g546050.t1.2), 4-(cytidine 5'-diphospho)-2-C-methyl-D-erythritol kinase (CMK, Cre02.g145050.t1.2), 2-C-methyl-D-erythritol 2,4-cyclodiphosphate synthase (MDS, Cre12.g503550.t1.2) and isopentenyl-diphosphate delta-isomerase (IDI, Cre08.g381800.t1.1). Two isoforms of *IDI* are predicted to be present in *C. reinhardtii*, but only one was successfully amplified in this case. Concentration of MeJA up to 0.5 mM did not have a significant effect on transcript levels, while the highest concentration of MeJA (1 mM) triggered a clear up-regulation of the genes encoding five key enzymes (Table A1, Figure 3A). Importantly, the over-expression of genes encoding the enzymes up-stream of MEP formation are matched by expression levels of transcripts encoding enzymes downstream of MEP to avoid pathway bottlenecks, especially the “gatekeeper” enzymes DXS and IDI.

DXS and HDR, and to some extent DXR, are known to play a major role in the control of flux in the MEP pathway of higher plants [11, 47, 48]. Transgenic *Arabidopsis* plants that over- or underexpress DXS respectively accumulated more or less isoprenoids (chlorophylls, tocopherols, carotenoids, abscisic acid, and gibberellins) compared with wild-type plants [49], demonstrating that DXS catalyzes one of the rate-limiting steps of the MEP biosynthetic pathway. In addition to DXS, DXR and HDR enzymes also showed rate-limiting roles in IPP

and DMAPP synthesis [47]. However, unlike DXS, the regulation of these two enzymes appears to vary among plants and in different conditions. As of today, DXS represents the most obvious target for the manipulation of the isoprenoid metabolism. Enfissi et al. [50] demonstrated a 1.6-fold increase in the carotenoid content of transgenic tomato lines containing a bacterial *dxs* targeted to the plastid, while a 7-fold increase in phytoene was reported in potato tubers engineered with a bacterial *dxs* gene [51]. Lauersen et al. [12] observed similar results in *C. reinhardtii* with the expression of an heterologous DXS (from *Salvia pomifera*), which increased flux towards heterologous diterpenoids through the MEP pathway. However, simultaneous expression of DXS and the downstream enzyme geranylgeranyl pyrophosphate synthase (GGPPS) as a fusion protein had a similar effect to overproduction of either target alone, suggesting that the cell has a natural tolerance to increased flux through the MEP pathway as long as there is a sink for the end product [12]. The over-expression of heterologous diterpene synthase did not outcompete native mechanisms for GGPP channeling, as the levels of downstream carotenoids and chlorophylls were unchanged [12]. These results indicate that the cell has other mechanisms in place to compensate for modifications in the MEP pathway than transcriptional up-regulation. In other words, small variations in transcript abundances may change flux ratios, but when the cell is responding to a stress other regulations mechanisms such as post-translational regulations can play a major role. In higher plants mutants affected in any particular step of the MEP pathway, low transcript levels of the pathway genes correlates with the low abundance of the corresponding enzymes, except for the DXS and HDR proteins, strongly suggesting a post-translational regulatory mechanism for these two enzymes [47, 48]. Also, the current study looked mostly at changes in transcripts level following MeJA treatment, regulation at the post-translational level should not be excluded. Especially for DXS, the non-significant

change in *dxs* transcript level after treatment with 1 mM MeJA (Figure 3A) could suggest that the regulation happened at a post-translational level.

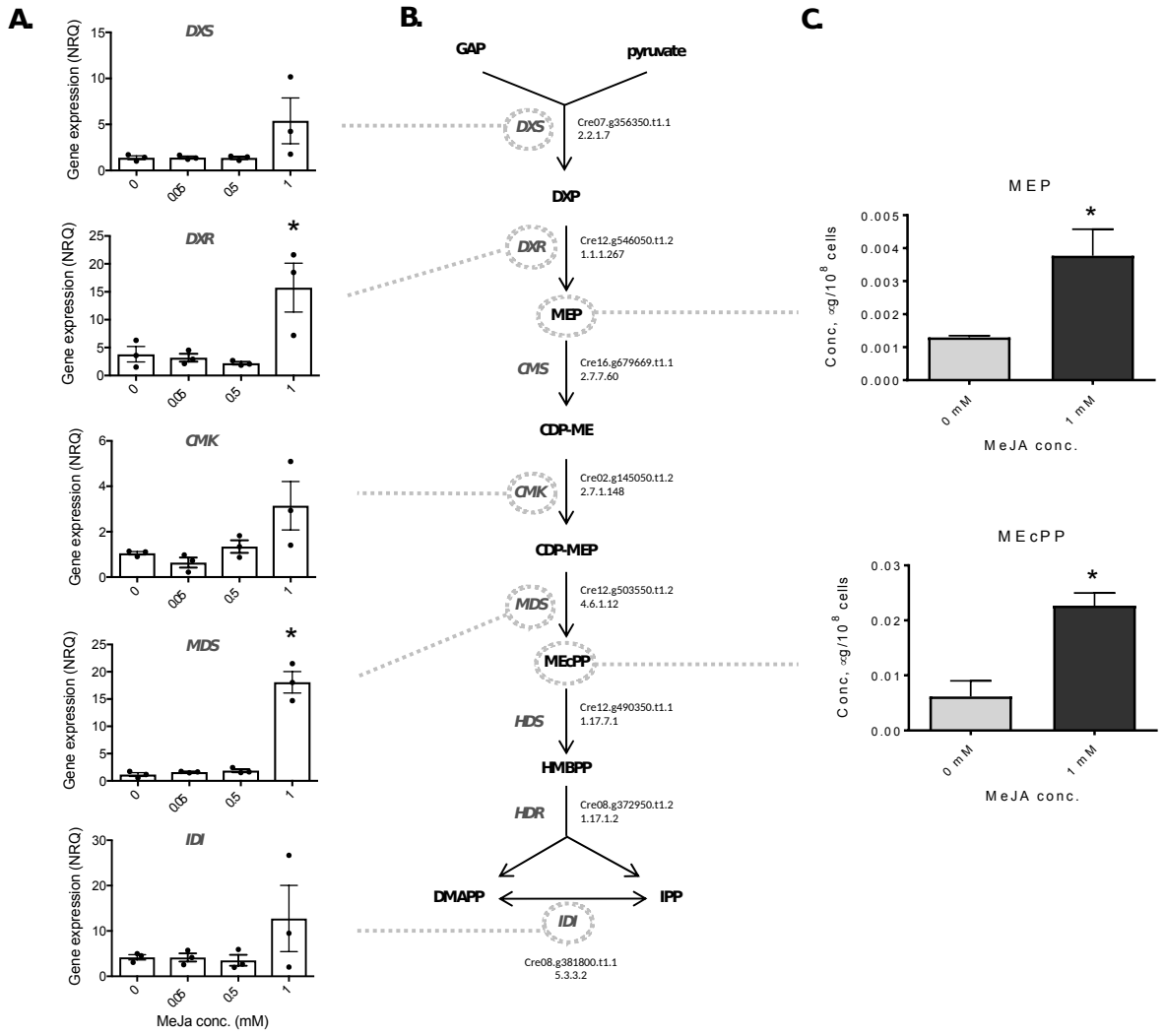

Figure 3. **Effect of MeJA on the MEP pathway of *C. reinhardtii* after 48 hours of treatment**. **A.** Relative expression level (Normalized relative quantity, NRQ) of five genes of the MEP pathway in cells treated with 0, 0.05, 0.5 and 1 mM of MeJA, Mean ± SEM, n=3, each dot represent a sample. *Significant difference (Dunnett's, $P<0.05$) between the control (0 mM) and the treatment at 48 hours. **B.** Schematic of the MEP pathway. **C.** Concentrations of two intermediates in 10^8 cells treated with 0 and 1 mM of MeJA for 48 hours. Lower

concentrations of MeJA were not investigated here as they did not affect the gene expression. Mean ± SEM is shown (n = 3) and unpaired *t*-test determine statistical significance between the control (0 mM) and the 1 mM treatment ($p < 0.05$ [*]). GAP: D-glyderaldehyde 3-phosphate; *DXS*: 1-deoxy-D-xylulose 5-phosphate synthase gene; DXP: 1-deoxy-D-xylulose 5-phosphate; *DXR*: 1-deoxy-D-xylulose 5-phosphate reductoisomerase gene; MEP: 2-C-methyl-D-erythritol 4-phosphate; *CMS*: 2-C-methyl-D-erythritol 4-phosphate cytidylyltransferase gene; CDP-ME: 4-(cytidine 5'-diphospho)-2-C-methyl-D-erythritol; *CMK*: 4-(cytidine 5'-diphospho)-2-C-methyl-D-erythritol kinase gene; CDP-MEP: 2-phospho-4-(cytidine 5'-diphospho)-2-C-methyl-D-erythritol; *MDS*: 2-C-methyl-D-erythritol 2,4-cyclodiphosphate synthase gene; MEcPP: 2-C-methyl-D-erythritol-2,4-cyclodiphosphate; *HDS*: (E)-4-hydroxy-3-methylbut-2-enyl-diphosphate synthase gene; HMBPP: 1-hydroxy-2-methyl-2-(E)-butenyl 4-diphosphate; *HDR*: 4-hydroxy-3-methylbut-2-enyl diphosphate reductase gene; DMAPP: Dimethylallyl diphosphate; IPP: Isopentenyl diphosphate; *IDI*: Isopentenyl-diphosphate Delta-isomerase gene.

3.4. Effect of MeJA on MEP pathway intermediates, prenyl phosphates and pigments

The increase in gene expression was correlated with an increase in abundance of 2-C-methyl-D-erythritol 4-phosphate (MEP) and 2- C-methyl-D-erythritol-2,4-cyclodiphosphate (MEcPP), with significantly higher concentrations observed in the MeJA-treated cells than in that of the control (Table A1, Figure 3C). MEP and MEcPP play a central role in the regulation of the MEP pathway and stress response in plants [52, 53]. In the plastids of higher plant cells, MEP is the first committed precursor of the pathway and activates the expression of *MDS* gene [52, 54]. MDS produces MEcPP, which also acts as retrograde signalling

molecule that directly or indirectly coordinates the expression of nuclear genes encoding plastid-localized proteins in plants [53]. This MEcPP mediated signalling activity is transient and can occur only under specific abiotic stresses [52]. The transporter responsible for the transport of plastid-localized MEcPP to the nucleus has not yet been identified in plants [55], however, it is known for bacteria [56]. Overall, we provide evidence of a marked up-regulation of the MEP pathway in both transcripts and metabolites following treatment with MeJA (Figure 3).

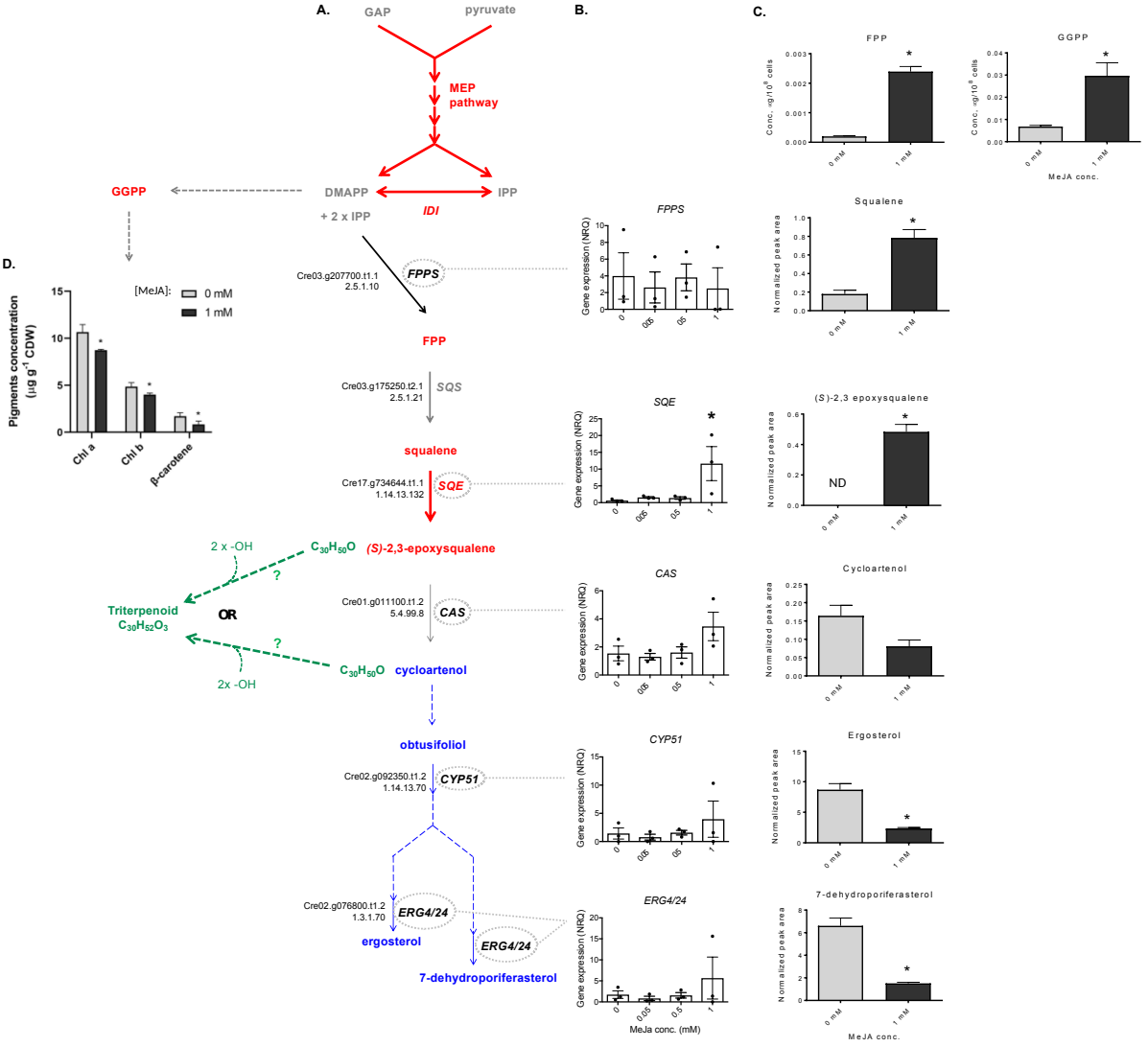

Figure 4. Effect of MeJA on triterpenoid biosynthesis. A. Conceptual diagram of the effect of MeJA on the putative triterpenoid pathway of *C. reinhardtii*. The metabolites and genes

proven (in this study) to be over-expressed are displayed in red, the downregulated metabolites are in blue. The genes not showing significant regulation are displayed in black. Dashed arrows indicate multiple enzymatic steps. An uncharacterised pathway branch (in green) hypothetically stems from either (*S*)-2,3-epoxysqualene or cycloartenol steps. **B.** Relative expression level of *SQE*, *CAS*, *CYP51* and *ERG4/24* in cells treated with 0, 0.05, 0.5 and 1 mM of MeJA for 48 hours. Mean ± SEM (n = 3). **C.** Relative quantity of squalene, (*S*)-2,3-epoxysqualene, cycloartenol, ergosterol and 7-dehydroporiferasterol in the control (0 mM) and the treated cells (1 mM) after 48 hours. ND = Not Detected. Mean ± SEM is shown (n = 3) and unpaired *t*-test determine statistical significance between the control (0 mM) and the 1 mM treatment ($p < 0.05$ [*]). **D.** Pigment concentrations in control (0 mM) and 1 mM MeJA treated cells after 48 hours of treatment. Mean ± SEM is shown (n = 3) and unpaired *t*-test determine statistical significance between the control (0 mM) and the 1 mM treatment ($p < 0.05$ [*]). GAP: D-glyderaldehyde 3-phosphate; DMAPP: Dimethylallyl diphosphate; IPP: Isopentenyl diphosphate; *IDI*: Isopentenyl-diphosphate Delta-isomerase gene, *FPPS*: farnesyl diphosphate synthase gene; *GGPPS*: geranylgeranyl pyrophosphate synthase gene; GGPP: geranylgeranyl pyrophosphate; FPP: farnesyl pyrophosphate; *SQS*: squalene synthase gene, *SQE*: squalene epoxidase gene; *CAS*: cycloartenol synthase gene; *CYP51*: sterol C-14 demethylase gene; *EGR4/24*: delta14-sterol reductase gene.

The shift in metabolism towards the production of DMAPP and IPP suggests a possible accumulation of the prenyl phosphates geranyl pyrophosphate (GPP), geranylgeranyl pyrophosphate (GGPP) and farnesyl pyrophosphate (FPP) in the cells treated with MeJA. While GPP was not detected in the samples, the concentrations of FPP and GGPP were significantly higher in the treated cells compare with the control (Figure 4C). *C. reinhardtii* possesses at least one putative GPP synthase (Cre12.g511700), suggesting that GPP is

probably present at concentration too low to be detected. The increase in accumulation of GGPP in treated *C. reinhardtii* implies an effect of MeJA on the synthesis of diterpenoids, carotenoids and phytoenes. However, the concentrations of chlorophyll a, b and β-carotene were lower in the treated cells than in the controls (Figure 4D). These results correlate with the decrease in the photosynthetic activity of photosystem II observed previously (Figure 2B) and illustrate the diversion of IPP and DMAPP away from chlorophylls and β-carotene towards biosynthesis of sterols and/or other pigments. The occurrence of a metabolic shift towards the formation of triterpenoid metabolites such as sterols is also supported by the dramatic increase in accumulation of FPP. The rest of this study focuses mainly on triterpenoid synthesis, starting with the analysis of the expression of the gene encoding the FPP synthase (FPPS, Cre03.g207700.t1.1). Despite the clear effect at the metabolite level, the expression of the *FPPS* gene was unaffected by the treatment with MeJA (Figure 4B). This suggests regulation at the translational or post-translational level, rather than at the transcriptional level, or that *Cre03.g207700.t1.1* does not encode a FPPS, since the function of this gene has never been experimentally proven in *C. reinhardtii*.

3.5. Accumulation of triterpenoid precursors and decrease in main sterols abundance in MeJA-elicited cells

C. reinhardtii membranes contain ergosterol and 7-dehydroporiferasterol as main sterols and these are synthesised from squalene, through the formation of cycloartenol, by a pathway that resembles that of higher plants [57]. Squalene, the C30 precursor of triterpenoids, is the result of the condensation of two FPP molecules (Figure 4A). Targeted analyses showed a four-fold accumulation of squalene in the elicited-cells (1 mM MeJA) compared to the control 48 hours after treatment (Figure 4C). The increase in squalene was correlated with the increased

accumulation of *(S)*-2,3-epoxysqualene and the up-regulation of the gene encoding squalene epoxidase (*SQE*, *Cre17.g734644.t1.1*), the enzyme catalysing the oxidization of squalene in *(S)*-2,3-epoxysqualene (Figure 4).

Although the increased accumulation of squalene in *C. reinhardtii* cells following MeJA treatment was previously reported [25], the present study is the first to demonstrate the effect of MeJA on the up-regulation of *SQE* transcripts in *C. reinhardtii*. According to BLAST searches and knockdown experiments [35], *C. reinhardtii* only has one conventional SQE (CrSQE), which differs from diatoms and other microalgae. These organisms have recently been determined to use an alternative SQE (AltSQE, [27]). SQE is an important point of regulation and rate-limiting step in sterol and triterpenoid biosynthesis [58]. According to the current literature, most plants have two or more copies of *SQE* genes [58]. In *Panax ginseng*, the two *SQE* genes (*PgSQE1* and *PgSQE2*) have been shown to be differentially regulated by MeJA treatment [58]. While MeJA enhanced the expression of the *PgSQE1* gene, which is suspected to contribute to ginsenoside biosynthesis, it did not affect the expression of *PgSQE2* gene involved in phytosterol production. Similarly, in *Medicago truncatula*, one squalene epoxidase gene (*MtSQE2*) was up-regulated by treatment with MeJA leading to the accumulation of triterpenes, while the sterol composition and the second squalene epoxidase gene (*MtQSE1*) remained unaffected [59]. In this study, we showed that *CrSQE* expression is sensitive to MeJA.

In MeJA treated *C. reinhardtii* cultures, the increased accumulation of *(S)*-2,3-epoxysqualene was correlated with a decrease in the abundance of the key sterol intermediate cycloartenol, a direct product of the cyclisation of *(S)*-2,3-epoxysqualene catalysed by the cycloartenol synthase (CAS) enzyme, and the two main sterols of *C. reinhardtii*, ergosterol and 7-

dehydroporiferasterol (Figure 4). Surprisingly, we detected yet uncharacterised triterpenoid-based molecules in samples treated with MeJA (Figure 5). These compounds eluted at Rt 24.2 min (m/z 461) and 25.0 min (m/z 461). High resolution mass spectrometry (HRMS) and fragmentation pattern were indicative of compounds with molecular formula $C_{30}H_{52}O_3$, possibly two different isomers (Figure A2). The chemical formula and mass spectrum correspond to protopanaxadiol-type triterpene saponins, which have been shown to be over-produced in *Panax ginseng* roots treated with MeJA [60, 61]. The peaks were compared to the analytical standard of protopanaxodiol, but the latter eluted at a different retiention time (Figure 5). More work is currently been undertaken to elucidate the structure of these triterpenoid-based molecules. The mass spectrum (Figure A2) reveals that the molecule contains three hydroxyl groups and is likely to be derived from the double hydroxylation of either the (*S*)-2,3-epoxysqualene - as in the case of saponin biosynthesis - or cycloartenol. Both (*S*)-2,3-epoxysqualene and cycloartenol have the same chemical formula ($C_{30}H_{50}O$) and a mass of 426 Daltons, which is two hydroxyl groups away from the 460 Daltons molecule. The simultaneous increase in *(S)*-2,3-epoxysqualene and decrease in cycloartenol content coupled with the accumulation of this new triterpenoid compounds suggests a hypothetical pathway branching that uses either (*S*)-2,3-epoxysqualene or cycloartenol as a substrate (Figure 4). To outline the presence of a putative branching node, the expression of key sterol genes in *C. reinhardtii* were analysed. Expression data of *CAS* (Cre01.g011100.t1.2), sterol C-14 demethylase (*CYP51*, Cre02.g092350.t1.2), and delta14-sterol reductase (*EGR4/24*, Cre02.g076800.t1.2) genes did not show a clear down or up-regulation as no significant differences with the control (0 mM) were observed (Figure 4B, Table A1). These inconclusive results did not provide sufficient transcriptomic clues to determine whether the pathway branching occurs right after the conversion of squalene to *(S)*-2,3-epoxysqualene or after the conversion of the latter to cycloartenol.

Numerous studies performed on higher plants show the same effect with an increased content of triterpenoids directly synthesized from *(S)*-2,3-epoxysqualene and an associated decrease in sterol synthesis downstream from cycloartenol after treatment with MeJA [59, 62, 63]. Mangas et al. (2006) previously reported that the induction of nor-seco-friedelane galphimines synthesis (triterpenoids derived from *(S)*-2,3-epoxysqualene) was coupled with the inhibition of sterol synthesis by MeJA in the plant *Centella asiatica* [62]. In the same plant elicited with MeJA, Kim et al. [63] showed an upregulation of β-amyrin synthase (CabAS), a key enzyme in the biosynthesis of triterpene saponins, and the downregulation of cycloartenol synthase gene (*CaCAS*). Furthermore, Suzuki et al. [59] reported an accumulation of saponins (triterpene aglycone) derived from β-amyrin, a product of the cyclization of *(S)*-2,3-epoxysqualene, and a significant reduction in *CAS* transcript levels following MeJA-elicitation of *Medicago truncatula*. MeJA seems to have a clear effect on triterpenoids accumulation and cycloartenol synthase downregulation in higher plants. Transposed to *C. reinhardtii*, these results could suggest that the branching pathway uses *(S)*-2,3-epoxysqualene as substrate.

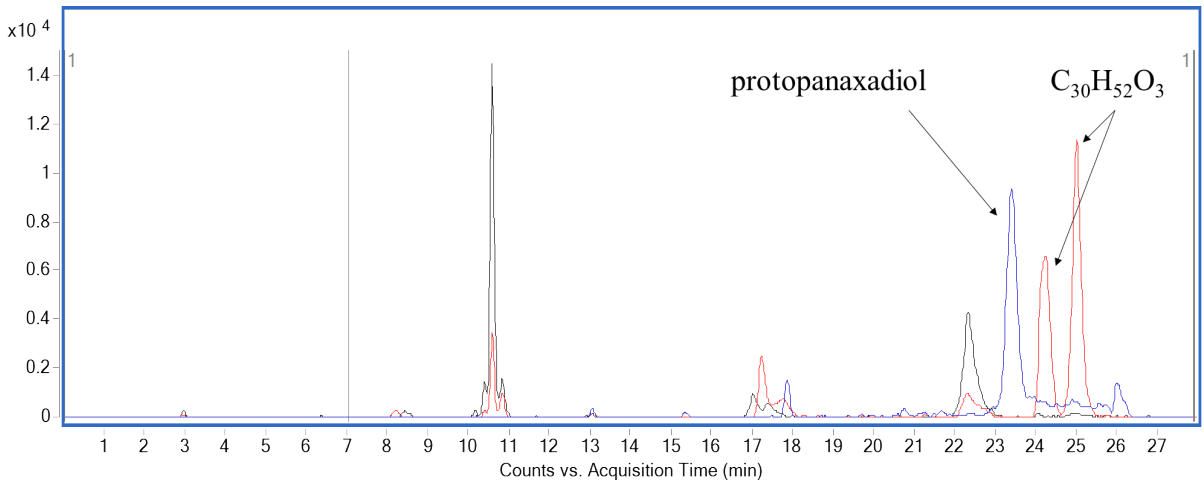

Figure 5. Detection of uncharacterised triterpenoid-based molecules in MeJA-treated cells. Overlay of LC-MS chromatograms showing the accumulation of two triterpenoid-based

molecules of same formula ($C_{30}H_{52}O_3$) in the *C. reinhardtii* cells treated with 1 mM of MeJA (red) compared to the untreated cells (black) at 48 hours and the protopanaxadiol standard (blue). Data from one representative sample out of 3 biological replicates.

3.6. Effect of growth conditions on isoprenoid metabolic flux

Among environmental factors, light appears to have the most profound effect on the control of MEP-pathway flux [48]. In *A. thaliana*, light induces the accumulation of transcripts from the MEP-pathway genes and genes encoding enzymes of downstream pathways, such as carotenoid and chlorophyll biosynthesis [48]. Furthermore, the expression of *AtDXS* and *AtHDR* follows a circadian pattern, with levels of transcripts increasing and decreasing at day and night-time respectively [48]. In *C. reinhardtii*, the production of an heterologous diterpenoid (13R(+) manoyl oxide) in the chloroplast was higher in photoautotrophic conditions (CO_2 as sole carbon source) in day:night illumination cycles than in continuous light [12]. The production of the sesquiterpene biodiesel precursor (E)-α-bisabolene in the cytosol also showed to benefit from light:dark cycles, but mixotrophy (with acetate) yielded three times more bisabolene than autotrophy [13]. Environmental factors seem to affect the production of terpenoids depending on their localization within the cell, with the production of diterpenes in chloroplast being affected by light, while the production of sesquiterpenes in the cytosol is influenced by the carbon source. Lauersen et al. [9] observed that the abundance of FPP varies in *C. reinhardtii* depending on the carbon-regime, in this case acetate or CO_2. Therefore, the production of native triterpenoids in *C. reinhardtii* is likely to be affected, to some extend, by the growth conditions. The transcriptomic datasets available on Phytozome (https://phytozome.jgi.doe.gov) showed that the target genes investigated in this study are differently regulated under different growth conditions (Supplementary Table A2), with some genes showing higher variations than others. Unfortunately, we cannot directly relate these

regulations to our findings because (i) qPCR data and FPKM values are not directly comparable and (ii) most of datasets on Phytozome lack precise information about experimental conditions. The current study was conducted in mixotrophy (acetate) at constant low-light (up to 50 µmol photon m^{-2} s^{-1}). Some could argue that due to the difference in cell density between the control and the treatment after addition of MeJA, the growth conditions in the control and the treatment are slightly different (e.g. light exposure per cell) and could therefore influence the differences observed in metabolites concentrations. To address this question, future works will investigate the production of triterpenoids when the cells are exposed to high-light (over 300 µmol photon m^{-2} s^{-1}) or under photoautotrophic conditions and compare to the concentrations obtained under MeJA-elicitation. Ultimately, photoautotrophy (i.e. using light and CO_2 as sole inputs) is the preferred condition for commercial production of terpenoid in a sustainable manner.

Finally, as a future perspective, it would be interesting to assess the productivity of *C. reinhardtii* strains engineered to produce each sesqui-, di-, and tri-terpenoids upon MeJA treatment. While strains producing heterologous sesqui- and di-terpenoids are already available [9, 12], *C. reinhardtii* strains producing heterologous triterpenoids could be created as shown in *P. tricornutum* [10].

4. CONCLUSIONS

This study showed that a 48 h-treatment of *C. reinhardtii* cells with 1 mM of MeJA arrested the growth and significantly impaired the photosynthetic activity, while up-regulating the MEP pathway leading to the accumulation of the triterpenoids precursors farnesyl pyrophosphate, squalene and (*S*)-2,3-epoxysqualene. This increase in (*S*)-2,3-epoxysqualene

was associated with a decrease in cycloartenol and main sterols of *C. reinhardtii*. Coupling metabolite profiling of elicitor-treated microalgae cells with gene expression analysis lead to new understandings in the regulation of isoprenoids and triterpenoids. This study also brought new insights in MeJA signalling, which is central in plant sciences. We suggested that the signalling mechanisms evolved independently, since *C. reinhardtii* seems to lack orthologs of key genes involved in MeJA signalling in plants. We provided evidence of the accumulation of a novel, likely specialised and uncharacterised triterpenoid secondary metabolite, and hypothesized the presence of a specialised pathway branching just upstream of cycloartenol. Further research is necessary and currently ongoing in our laboratory to identify and characterise metabolites and enzymes involved in this hypothetical metabolic branching in the triterpenoid metabolism of *C. reinhardtii.* This work represents one of the first efforts aimed at elucidating the regulation of terpenoid metabolism in *C. reinhardtii*, which is the most common model organism for algal biology and biotechnology. The knowledge generated by this work sets the basis for more detailed gene discovery experiments that will guide metabolic engineering and synthetic biology approaches for the heterologous production of terpenoids in algae.

CONFLICT OF INTEREST

The authors declare no conflict of interest.

ACKNOWLEDGEMENTS

This work was supported by funding from the Climate Change Cluster (C3) of the University of Technology Sydney (UTS, Australia). MF is supported by a CSIRO Synthetic Biology Future Science Platform Fellowship, co-funded by UTS and CSIRO (Australia). The authors would like to thank Associate Professor Claudia Vickers (The University of

Queensland, Australia) for sharing standards and technical advices on MEP pathway metabolites analysis.

AUTHOR'S CONTRIBUTIONS

A.S.C. and M.F. conceived and designed the study; A.S.C. and M.F. performed the research; U.K. acquired and analysed the chemistry data; J.A. extracted the RNA; A.S.C. and M.P. analysed qPCR data and performed statistical analysis; P.J.R. funded the research; A.S.C wrote the manuscript with inputs from M.F., U.K., J.A., M.P. and P.J.R.

SUPPLEMENTARY MATERIAL

The BLASTp analysis was run against Phytozome using the following sequences as query:

>AT2G39940.1 [COI1]
MEDPDIKRCKLSCVATVDDVIEQVMTYITDPKDRDSASLVCRRWFKIDSETREHVTMALCYTATPDRLSRRFPNLRSLKLKGKPRA
AMFNLIPENWGGYVTPWVTEISNNLRQLKSVHFRRMIVSDLDLDRLAKARADDLETLKLDKCSGFTTDGLLSIVTHCRKIKTLLME
ESSFSEKDGKWLHELAQHNTSLEVLNFYMTEFAKISPKDLETIARNCRSLVSVKVGDFEILELVGFFKAAANLEEFCGGSLNEDIGM
PEKYMNLVFPRKLCRLGLSYMGPNEMPILFPFAAQIRKLDLLYALLETEDHCTLIQKCPNLEVLETRNVIGDRGLEVLAQYCKQLK
RLRIERGADEQGMEDEEGLVSQRGLIALAQGCQELEYMAVYVSDITNESLESIGTYLKNLCDFRLVLLDREERITDLPLDNGVRSLLI
GCKKLRRFAFYLRQGGLTDLGLSYIGQYSPNVRWMLLGYVGESDEGLMEFSRGCPNLQKLEMRGCCFSERAIAAAVTKLPSLRYL
WVQGYRASMTGQDLMQMARPYWNIELIPSRRVPEVNQQGEIREMEHPAHILAYYSLAGQRTDCPTTVRVLKEPI

>AT1G19180.1 [JAZ1]
MSSSMECSEFVGSRRFTGKKPSFSQTCSRLSQYLKENGSFGDLSLGMACKPDVNGTLGNSRQPTTTMSLFPCEASNMDSMVQDVK
PTNLFPRQPSFSSSSSSLPKEDVLKMTQTTRSVKPESQTAPLTIFYAGQVIVFNDFSAEKAKEVINLASKGTANSLAKNQTDIRSNIATI
ANQVPHPRKTTTQEPIQSSPTPLTELPIARRASLHRFLEKRKDRVTSKAPYQLCDPAKASSNPQTTGNMSWLGLAAEI

>At1g74950 [JAZ2]
MSSFSAECWDFSGRKPSFSQTCTRLSRYLKEKGSFGDLSLGMTCKPDVNGGSRQPTMMNLFPCEASGMDSSAGQEDIKPKTMFPR
QSSFSSSSSSGTKEDVQMIKETTKSVKPESQSAPLTIFYGGRVMVFDDFSAEKAKEVIDLANKGSAKSFTCFTAEVNNNHSAYSQKEI
ASSPNPVCSPAKTAAQEPIQPNPASLACELPIARRASLHRFLEKRKDRITSKAPYQIDGSAEASSKPTNPAWLSSR

>AT3G17860 [JAZ3]
MERDFLGLGSKNSPITVKEETSESSRDSAPNRGMNWSFSNKVSASSSQFLSFRPTQEDRHRKSGNYHLPHSGSFMPSSVADVYDSTR
KAPYSSVQGVRMFPNSNQHEETNAVSMSMPGFQSHHYAPGGRSFMNNNNNSQPLVGVPIMAPPISILPPPGSIVGTTDIRSSSKPIGS
PAQLTIFYAGSVCVYDDISPEKAKAIMLLAGNGSSMPQVFSPPQTHQQVVHHTRASVDSSAMPPSFMPTISYLSPEAGSSTNGLGAT
KATRGLTSTYHNNQANGSNINCPVPVSCSTNVMAPTVALPLARKASLARFLEKRKERVTSVSPYCLDKKSSTDCRRSMSECISSSLS
SAT

>At1g72450 [JAZ6]
MSTGQAPEKSNFSQRCSLLSRYLKEKGSFGNINMGLARKSDLELAGKFDLKGQQNVIKKVETSETRPFKLIQKFSIGEASTSTEDKAI
YIDLSEPAKVAPESGNSQLTIFFGGKVMVFNEFPEDKAKEIMEVAKEANHVAVDSKNSQSHMNLDKSNVVIPDLNEPTSSGNNEDQ
ETGQQHQVVERIARRASLHRFFAKRKDRAVARAPYQVNQHGSHLPPKPEMVAPSIKSGQSSQHIATPPKPKAHNHMPMEVDKKEG
QSSKNLELKL

>At5g13220 [JAZ10]
MSKATIELDFLGLEKKQTNNAPKPKFQKFLDRRRSFRDIQGAISKIDPEIIKSLLASTGNNSDSSAKSRSVPSTPREDQPQIPISPVHASL
ARSSTELVSGTVPMTIFYNGSVSVFQVSRNKAGEIMKVANEAASKKDESSMETDLSVILPTTLRPKLFGQNLEGDLPIARRKSLQRF
LEKRKERLVSTSPYYPTSA

>AT1G70700 [JAZ9]
MERDFLGLSDKQYLSNNVKHEVNDDAVEERGLSTKAAREWGKSKVFATSSFMPSSDFQEAKAFPGAYQWGSVSAANVFRRCQFG
GAFQNATPLLLGGSVPLPTHPSLVPRVASSGSSPQLTIFYGGTISVFNDISPDKAQAIMLCAGNGLKGETGDSKPVREAERMYGKQIH
NTAATSSSSATHTDNFSRCRDTPVAATNAMSMIESFNAAPRNMIPSVPQARKASLARFLEKRKERLMSAMPYKKMLLDLSTGESSG
MNYSSTSPT

>At1g32640 [MYC2]
MTDYRLQPTMNLWTTDDNASMMEAFMSSSDISTLWPPASTTTTTATTETTPTPAMEIPAQAGFNQETLQQRLQALIEGTHEGWTY
AIFWQPSYDFSGASVLGWGDGYYKGEEDKANPRRRSSSPPFSTPADQEYRKKVLRELNSLISGGVAPSDDAVDEEVTDTEWFFLVS
MTQSFACGAGLAGKAFATGNAVWVSGSDQLSGSGCERAKQGGVFGMHTIACIPSANGVVEVGSTEPIRQSSDLINKVRILFNFDGG
AGDLSGLNWNLDPDQGENDPSMWINDPIGTPGSNEPGNGAPSSSSQLFSKSIQFENGSSSTITENPNLDPTPSPVHSQTQNPKFNNTF
SRELNFSTSSSTLVKPRSGEILNFGDEGKRSSGNPDPSSYSGQTQFENKRKRSMVLNEDKVLSFGDKTAGESDHSDLEASVVKEVAV
EKRPKKRGRKPANGREEPLNHVEAERQRREKLNQRFYALRAVVPNVSKMDKASLLGDAIAYINELKSKVVKTESEKLQIKNQLEE
VKLELAGRKASASGGDMSSSCSSIKPVGMEIEVKIIGWDAMIRVESSKRNHPAARLMSALMDLELEVNHASMSVVNDLMIQQATV
KMGFRIYTQEQLRASLISKIG

>AT4G02570 [CUL1]
MERKTIDLEQGWDYMQTGITKLKRILEGLNEPAFDSEQYMMLYTTIYNMCTQKPPHDYSQQLYDKYREAFEEYINSTVLPALREK
HDEFMLRELFKRWSNHKVMVRWLSRFFYYLDRYFIARRSLPPLNEVGLTCFRDLVYNELHSKVKQAVIALVDKEREGEQIDRALL
KNVLDIYVEIGMGQMERYEEDFESFMLQDTSSYYSRKASSWIQEDSCPDYMLKSEECLKKERERVAHYLHSSSEPKLVEKVQHELL
VVFASQLLEKEHSGCRALLRDDKVDDLSRMYRLYHKILRGLEPVANIFKQHVTAEGNALVQQAEDTATNQVANTASVQEQVLIRK
VIELHDKYMVYVTECFQNHTLFHKALKEAFEIFCNKTVAGSSSAELLATFCDNILKKGGSEKLSDEAIEDTLEKVVKLLAYISDKDL
FAEFYRKKLARRLLFDRSANDDHERSILTKLKQQCGGQFTSKMEGMVTDLTLARENQNSFEDYLGSNPAANPGIDLTVTVLTTGF
WPSYKSFDINLPSEMIKCVEVFKGFYETKTKHRKLTWIYSLGTCHINGKFDQKAIELIVSTYQAAVLLLFNTTDKLSYTEILAQLNLS
HEDLVRLLHSLSCAKYKILLKEPNTKTVSQNDAFEFNSKFTDRMRRIKIPLPPVDERKKVVEDVDKDRRYAIDAAIVRIMKSRKVLG
HQQLVSECVEQLSRMFKPDIKAIKKRMEDLITRDYLERDKENPNMFRYLA

Table A1. Analyse of variance using GraphPad Prism 5.0 software to test the dissimilarities in quantum yield, cell density, metabolites concentrations and differential expression of key metabolic genes in control and MeJA-treated cells of *Chlamydomonas reinhardtii*. Df = degrees of freedom; MS = mean sum of squares. Bold face indicates statistical significance ($P < 0.05$).

A. Two-way ANOVA and post-hoc Tukey's HSD test results for the quantum yield data.

Source of Variation	Df	MS	F	P value
Interaction	**6**	**0.007007**	**5.623**	**0.0026**
Time	2	0.003751	3.01	0.0777
Treatment	3	0.006066	1.189	0.3736

Tukey's multiple comparisons test

	Mean Diff.	Significant?	Summary	Adjusted P Value
0 hour				
0 mM vs. 0.05 mM	-0.01467	No	ns	0.9840
0 mM vs. 0.5 mM	0.002333	No	ns	>0.9999
0 mM vs. 1 mM	0.011	No	ns	0.9931
0.05 mM vs. 0.5 mM	0.017	No	ns	0.9756
0.05 mM vs. 1 mM	0.02567	No	ns	0.9231
0.5 mM vs. 1 mM	0.008667	No	ns	0.9966
12 hours				

0 mM vs. 0.05 mM	-0.01467	No	ns	0.9840
0 mM vs. 0.5 mM	-0.02533	No	ns	0.9258
0 mM vs. 1 mM	-0.03667	No	ns	0.8088
0.05 mM vs. 0.5 mM	-0.01067	No	ns	0.9937
0.05 mM vs. 1 mM	-0.022	No	ns	0.9495
0.5 mM vs. 1 mM	-0.01133	No	ns	0.9925
48 hours				
0 mM vs. 0.05 mM	-0.01633	No	ns	0.9782
0 mM vs. 0.5 mM	-0.02033	No	ns	0.9595
0 mM vs. 1 mM	**0.146**	**Yes**	**	**0.0082**
0.05 mM vs. 0.5 mM	-0.004	No	ns	0.9997
0.05 mM vs. 1 mM	**0.1623**	**Yes**	**	**0.0031**
0.5 mM vs. 1 mM	**0.1663**	**Yes**	**	**0.0025**

B. Two-way ANOVA and post-hoc Tukey's HSD test results for the cell density data.

Source of Variation	Df	MS	F	P value
Interaction	**6**	**1455234787037**	**7.161**	**0.0008**
Time	**2**	**15238243750000**	**74.99**	**<0.0001**
Treatment	**3**	**923230925926**	**8.057**	**0.0084**

Tukey's multiple comparisons test

	Mean Diff.	Significant?	Summary	Adjusted P Value
0 hour				
0 mM vs. 0.05 mM	283333	No	ns	0.8384
0 mM vs. 0.5 mM	-133333	No	ns	0.9791
0 mM vs. 1 mM	-304333	No	ns	0.8078
0.05 mM vs. 0.5 mM	-416667	No	ns	0.6178
0.05 mM vs. 1 mM	-587667	No	ns	0.3322
0.5 mM vs. 1 mM	-171000	No	ns	0.9577
12 hours				
0 mM vs. 0.05 mM	145333	No	ns	0.9733
0 mM vs. 0.5 mM	-62000	No	ns	0.9978
0 mM vs. 1 mM	180333	No	ns	0.9509
0.05 mM vs. 0.5 mM	-207333	No	ns	0.9281
0.05 mM vs. 1 mM	35000	No	ns	0.9996
0.5 mM vs. 1 mM	242333	No	ns	0.8913
48 hours				
0 mM vs. 0.05 mM	-210000	No	ns	0.9256
0 mM vs. 0.5 mM	530000	No	ns	0.4206
0 mM vs. 1 mM	**2210000**	**Yes**	****	**<0.0001**
0.05 mM vs. 0.5 mM	740000	No	ns	0.1591
0.05 mM vs. 1 mM	**2420000**	**Yes**	****	**<0.0001**
0.5 mM vs. 1 mM	**1680000**	**Yes**	***	**0.0003**

C. One-way ANOVA results for gene expression data at 48 hours of treatment with MeJA.

Genes	DF	MS	F	P value
DXS	3	12.04	2.554	0.1285
DXR	**3**	**122.1**	**7.5**	**0.0104**
CMK	3	3.652	3.821	0.0575
MDS	**3**	**204.8**	**67.3**	**<0.0001**

IDI	3	58.14	1.388	0.3151
FPPS	3	1.835	0.1236	0.9435
SQE	**3**	**82.48**	**4.253**	**0.0451**
CAS	3	2.999	2.634	0.1216
CYP51	3	5.834	0.664	0.5972
ERG4/24	3	14.3	0.7222	0.5664

Dunnett's multiple comparisons test (comparing the mean of each treatment with the mean of the control)

Genes	Mean Diff.	Significant?	Summary	Adjusted P Value
DXS				
0 mM vs. 0.05 mM	-0.02483	No	ns	>0.9999
0 mM vs. 0.5 mM	0.01389	No	ns	>0.9999
0 mM vs. 1 mM	-4.01	No	ns	0.1249
DXR				
0 mM vs. 0.05 mM	0.6167	No	ns	0.9950
0 mM vs. 0.5 mM	1.618	No	ns	0.9263
0 mM vs. 1 mM	**-11.94**	**Yes**	*	**0.0169**
CMK				
0 mM vs. 0.05 mM	0.4115	No	ns	0.9166
0 mM vs. 0.5 mM	-0.2937	No	ns	0.9659
0 mM vs. 1 mM	-2.09	No	ns	0.0737
MDS				
0 mM vs. 0.05 mM	-0.4692	No	ns	0.9749
0 mM vs. 0.5 mM	-0.7178	No	ns	0.9212
0 mM vs. 1 mM	**-16.91**	**Yes**	****	**<0.0001**
IDI				
0 mM vs. 0.05 mM	0.0567	No	ns	>0.9999
0 mM vs. 0.5 mM	0.6673	No	ns	0.9985
0 mM vs. 1 mM	-8.543	No	ns	0.3114
FPPS				
0 mM vs. 0.05 mM	1.362	No	ns	0.9469
0 mM vs. 0.5 mM	0.161	No	ns	>0.9999
0 mM vs. 1 mM	1.492	No	ns	0.9327
SQE				
0 mM vs. 0.05 mM	-0.9324	No	ns	0.9872
0 mM vs. 0.5 mM	-0.7546	No	ns	0.9931
0 mM vs. 1 mM	**-11.02**	**Yes**	*	**0.0381**
CAS				
0 mM vs. 0.05 mM	0.2353	No	ns	0.9857
0 mM vs. 0.5 mM	-0.06539	No	ns	0.9996
0 mM vs. 1 mM	-1.926	No	ns	0.1346
CYP51				
0 mM vs. 0.05 mM	0.6466	No	ns	0.9861
0 mM vs. 0.5 mM	-0.151	No	ns	0.9999
0 mM vs. 1 mM	-2.537	No	ns	0.6137
ERG4/24				
0 mM vs. 0.05 mM	0.9009	No	ns	0.9888
0 mM vs. 0.5 mM	0.1606	No	ns	>0.9999
0 mM vs. 1 mM	-3.942	No	ns	0.5909

D. Two-tailed unpaired *t*-test results testing dissimilarities in metabolites concentrations between control and treated cells (1mM MeJA) at 48 hours of treatment.

Metabolite	t (df)	P value
MEP	**t (4) = 3.069**	**0.0373**
MEcPP	**t (4) = 4.506**	**0.0108**
GGPP	**t (4) = 3.881**	**0.0178**
FPP	**t (4) = 12.99**	**0.0002**
Squalene	**t (4) = 6.144**	**0.0036**
cycloartenol	t (4) = 2.502	0.0666
ergosterol	**t (4) = 6.415**	**0.0030**
7-dehydroporiferasterol	**t (4) = 7.305**	**0.0019**

Table A2. FPKM values for genes of interest as reported in Phytozome.

Experiment group	Experiment Name	DXS	DXR	CMK	MDS	IDI	FPPS	SQE	CAS	CYP51	ERG4 /24
Anaerobiosis	CC-124 Dark anoxic .5 hour	93.9	38.972	12.026	67.159	47.594	20.093	14.499	11.011	13.382	6.272
	CC-124 Dark anoxic 6 hours	68.557	58.677	9.885	54.511	15.577	15.824	185.632	24.514	236.999	5.267
	CC-124 Light oxic	97.465	64.004	22.566	65.998	15.837	33.691	22.323	15.77	40.129	10.693
	crr1 Dark oxic .5 hour	108.694	40.884	7.106	45.291	23.251	11.596	12.99	7.518	8.624	4.938
	crr1 Dark oxic 6 hours (1)	109.284	45.444	6.619	40.26	21.247	10.044	11.277	11.047	10.553	5.793
	crr1 Dark oxic 6 hours (2)	90.498	37.926	7.312	31.419	18.384	11.096	10.371	8.948	12.24	6.392
	crr1 Light oxic (1)	115.436	57.161	16.202	61.872	16.365	27.095	14.637	8.76	26.43	11.791
	crr1 Light oxic (2)	125.261	63.474	16.536	67.366	19.297	20.589	15.021	8.507	23.114	10.663
	crr1:CRR1 Dark anoxic .5 hour (1)	91.519	38.873	8.618	40.816	21.106	12.608	13.321	5.935	8.147	4.292
	crr1:CRR1 Dark anoxic .5 hour (2)	74.324	30.533	8.085	36.031	19.009	13.51	13.239	6.741	13.426	6.787
	crr1:CRR1 Dark anoxic 6 hours (1)	90.585	62.397	4.006	59.431	9.268	14.73	22.066	6.494	16.286	6.734
	crr1:CRR1 Dark anoxic 6 hours (2)	96.468	43.308	5.717	40.786	18.089	10.131	54.256	13.736	37.194	4.145
	crr1:CRR1 Light oxic (1)	91.236	52.824	14.882	66.517	16.409	23.368	15.501	8.984	25.058	11.994
	crr1:CRR1 Light oxic (2)	108.981	62.09	16.924	63.15	15.619	19.019	15.177	8.285	22.41	9.683
	crr1dCys Dark anoxic .5 hour (1)	82.715	33.924	7.297	43.421	22.778	13.49	11.507	6.642	13.312	7.148
	crr1dCys Dark anoxic .5 hour (2)	81.715	32.186	8.977	40.994	22.47	16.343	10.853	6.88	15.394	7.041
	crr1dCys Dark anoxic 6 hours (1)	93.594	42.759	11.415	52.198	18.916	13.399	13.058	9.604	23.857	7.238
	crr1dCys Dark anoxic 6 hours (2)	95.519	50.635	11.108	68.242	18.103	15.003	13.846	10.797	36.318	7.753
	crr1dCys Light oxic (1)	106.146	56.946	16.078	78.432	23.632	23.289	16.036	9.863	27.252	15.554
	crr1dCys Light oxic (2)	102.972	53.802	17.731	70.258	21.39	28.184	15.175	9.498	30.78	15.104
Bilin Signaling	4A+ 0 mM,0.5h white light (1)	254.607	85.813	9.855	117.231	96.502	45.399	80.269	38.73	84.341	50.41
	4A+ 0 mM,0.5h white light (2)	249.82	84.871	8.264	114.255	94.83	45.608	84.512	40.579	85.569	51.184
	4A+ 0 mM,dark (1)	107.473	46.216	10.984	29.458	11.427	28.109	18.051	10.908	34.65	8.184
	4A+ 0 mM,dark (2)	102.505	43.87	8.576	27.505	10.902	25.693	17.005	10.532	31.249	6.257
	4A+ 0.1 mM BV IXa,0.5h white light (1)	222.203	73.755	6.834	85.376	63.026	31.655	82.356	37.375	118.737	38.875

	4A+ 0.1 mM BV IXa,0.5h white light (2)	233.811	75.885	6.219	86.228	66.548	35.657	71.77	39.592	126.38	41.009
	4A+ 0.1 mM BV IXa,dark (1)	96.49	40.743	8.042	23.596	11.748	20.833	20.541	10.401	26.061	6.367
	4A+ 0.1 mM BV IXa,dark (2)	92.328	40.085	7.12	23.977	10.847	22.029	18.571	9.205	25.774	6.961
	hmox1 0 mM,0.5h white light (1)	140.701	72.741	8.585	74.657	60.112	39.92	60.767	24.216	76.397	29.479
	hmox1 0 mM,0.5h white light (2)	146.772	71.506	8.106	70.017	58.841	38.39	60.673	24.008	78.39	30.799
	hmox1 0 mM,dark (1)	88.789	44.346	8.829	30.012	17.056	29.526	20.501	9.568	37.037	7.338
	hmox1 0 mM,dark (2)	90.909	45.98	8.526	29.553	16.122	24.224	20.714	9.701	34.759	7.441
	hmox1 0.1 mM BV IXa,0.5h white light (1)	134.564	64.102	8.217	63.176	44.514	37.485	50.24	22.972	90.323	22.575
	hmox1 0.1 mM BV IXa,0.5h white light (2)	144.556	65.175	7.567	64.189	46.251	33.481	52.97	25.011	99.977	22.21
	hmox1 0.1 mM BV IXa,dark (1)	84.376	43.01	6.955	33.643	15.503	23.104	22.722	9.508	34.276	6.736
	hmox1 0.1 mM BV IXa,dark (2)	85.868	47.487	8.376	30.422	15.98	23.178	22.275	9.705	34.758	7.407
Cu Deficiency Photoautotrophic	WT-2137 Copper deficient (Minimal media) 3	143.678	58.931	9.928	51.578	10.126	16.962	71.086	12.155	39.409	8.427
	WT-2137 Copper deficient (TAP) 5	158.642	81.856	14.301	98.456	18.068	30.729	89.865	17.509	175.773	21.38
	WT-2137 Copper deficient (TAP) 6	145.907	71.424	22.333	110.119	23.416	31.982	104.775	25.513	183.672	18.071
	WT-2137 Copper deficient (TAP) 7	109.144	83.117	21.104	106.203	17.331	28.205	106.566	18.759	140.639	18.991
	WT-2137 Copper sufficient (Minimal media) 1	137.187	58.762	12.703	63.151	10.569	17.856	16.481	7.415	21.017	8.151
	WT-2137 Copper sufficient (Minimal media) 3	133.564	52.858	11.797	59.386	12.468	20.317	17.596	7.796	23.473	9.045
	WT-2137_Copper deficient (Minimal media) 1	105.652	31.486	7.906	33.59	9.905	16.384	68.73	12.061	58.952	8.272
	WT-2137_Copper deficient (TAP) 10	105.754	74.668	20.513	105.763	19.184	29.897	112.212	20.081	145.642	17.243
	WT-2137_Copper deficient (TAP) 8	115.638	81.522	23.887	106.797	20.271	32.665	103.911	22.073	130.105	13.778
	WT-2137_Copper deficient (TAP) 9	111.442	76.722	21.823	106.856	16.313	29.745	113.236	17.774	142.442	16.362
	WT-2137_Copper sufficient (TAP) 10	123.001	95.263	27.283	108.094	15.526	35.722	17.41	12.687	29.248	15.518
	WT-2137_Copper sufficient (TAP) 3	169.302	93.73	35.178	130.859	24.659	45.124	16.087	13.653	41.276	23.551
	WT-2137_Copper sufficient (TAP) 5	174.76	114.979	15.114	114.48	20.902	38.501	11.545	14.598	32.54	20.938
	WT-2137_Copper sufficient (TAP) 6	165.877	98.861	25.353	109.15	17.734	37.51	15.355	13.992	37.67	22.006
	WT-2137_Copper sufficient (TAP) 7	126.431	102.378	25.547	109.438	15.468	33.625	14.576	13.663	28.972	17.446
	WT-2137_Copper sufficient (TAP) 8	125.103	104.137	23.977	102.806	14.381	28.216	17.56	12.779	30.772	21.702
	WT-2137_Copper sufficient (TAP) 9	115.352	107.999	27.536	118.052	13.737	32.268	18.967	14.251	30.066	18.377
	crr1-2 Copper deficient (TAP) 3	94.523	64.352	24.664	49.22	11.147	27.165	45.152	11.135	40.016	10.022
	crr1-2 Copper deficient (TAP) 4	95.945	79.926	29.655	43.829	9.847	30.682	45.261	14.987	32.357	10.966
	crr1:CRR1 Copper deficient (TAP) 1	109.851	41.579	21.502	46.53	11.698	31.97	10.935	5.053	13.766	13.727
	crr1:CRR1 Copper deficient (TAP) 2	110.606	39.579	26.511	47.968	12.246	31.091	11.179	5.257	14.129	13.493
Fe Deficiency	WT-2137 Fe replete (Minimal media) 1	145.233	37.791	8.247	46.189	19.572	16.581	16.462	11.443	21.048	16.473
	WT-2137 Fe replete (Minimal media) 2	137.086	41.75	7.035	47.452	19.332	15.164	17.385	10.844	20.932	11.472

	WT-2137 Fe replete (Minimal media) 3	140.476	45.822	4.46	50.931	23.303	15.271	15.794	12.436	19.223	12.975
	WT-2137 Fe replete (Minimal media) 4	137.085	45.063	4.462	49.25	23.586	14.255	19.391	12.241	17.89	12.72
	WT-2137 Fe replete (TAP) 1	101.912	27.588	14.528	42.023	29.716	35.699	16.893	10.835	26.952	20.222
	WT-2137 Fe replete (TAP) 2	90.594	31.243	9.96	44.283	32.188	33.899	14.85	9.857	30.391	18.221
	WT-2137 Fe-deficient (Minimal media) 1	135.963	35.12	4.289	47.059	23.264	17.852	16.735	10.543	18.662	13.503
	WT-2137 Fe-deficient (Minimal media) 2	134.279	37.964	6.091	39.706	20.272	16.241	21.087	10.419	17.871	11.304
	WT-2137 Fe-deficient (Minimal media) 3	129.846	37.993	6.632	47.797	21.414	19.705	12.162	10.567	21.08	12.97
	WT-2137 Fe-deficient (Minimal media) 4	127.912	39.474	6.705	40.959	21.561	19.592	13.283	10.916	21.322	14.901
	WT-2137 Fe-deficient (TAP) 1	77.148	20.25	6.97	25.393	28.162	38.091	13.192	9.253	30.233	20.991
	WT-2137 Fe-deficient (TAP) 2	78.413	25.028	12.416	32.941	24.838	36.526	14.232	11.502	36.347	14.758
	WT-2137 Fe-deficient (TAP) 3	82.119	24.344	11.045	35.884	25.267	33.658	15.105	10.23	35.262	18.055
	WT-2137 Fe-limited (Minimal media) 1	133.634	29.037	3.249	33.986	28.541	14.606	18.663	10.379	18.488	17.517
	WT-2137 Fe-limited (Minimal media) 2	128.205	30.109	3.588	37.21	27.333	14.707	18.543	11.754	16.285	13.675
	WT-2137 Fe-limited (Minimal media) 3	113.909	25.679	1.919	32.138	30.616	16.6	17.413	10.58	16.164	15.698
	WT-2137 Fe-limited (Minimal media) 4	117.427	26.498	3.171	29.549	28.53	12.466	17.945	10.632	15.901	14.656
	WT-2137 Fe-limited (TAP) 1	118.755	50.129	7.672	43.877	51.806	31.552	10.271	14.113	21.493	16.676
	WT-2137 Fe-limited (TAP) 2	123.811	47.582	10.523	44.717	53.987	29.451	15.227	12.066	19.766	14.812
	WT-2137 Fe-limited (TAP) 3	148.422	48.11	9.142	39.12	59.664	26.286	15.5	11.98	22.708	18.649
GeneAtlas	Hetero.Ammonia	43.513	4.534	1.58	10.543	12.112	5.967	4.344	1.572	7.451	4.013
	Hetero.Ammonia Early	59.978	8.983	7.929	37.815	6.268	10.725	3.484	0.709	10.939	4.351
	Hetero.Ammonia MidLog	54.53	6.923	4.323	19.756	6.945	15.781	2.977	1.375	14.681	7.081
	Hetero.Nitrate	31.83	4.995	7.933	13.626	6.577	19.862	3.845	1.258	27.557	6.256
	Hetero.Urea	7.312	1	1.524	8.031	3.019	3.23	1.176	0.161	3.749	0.884
	Mixo.Ammonia	83.619	21.501	13.977	38.829	7.973	18.602	4.936	2.05	18.772	6.233
	Mixo.Ammonia Diurnal	127.897	38.39	29.874	85.09	3.94	17.474	3.77	1.897	14.768	7.663
	Mixo.Ammonia Early	72.552	14.7	11.725	36.868	18.19	13.983	5.072	1.895	15.525	6.601
	Mixo.Ammonia MidLog	80.766	19.486	15.078	40.218	7.958	18.292	4.624	1.647	21.268	6.425
	Mixo.HighLight Early	55.154	9.203	9.623	33.609	14.923	14.476	6.345	1.221	12.495	4.961
	Mixo.HighLight MidLog	67.66	7.69	10.154	55.461	11.374	11.488	5.686	0.777	11.265	5.667
	Mixo.Nitrate	74.716	22.384	15.742	35.74	6.165	21.388	4.011	1.653	24.764	6.954
	Mixo.Nitrate Diurnal	97.791	31.878	23.61	92.096	3.216	15.145	2.743	0.95	10.224	5.745
	Mixo.Urea Diurnal	111.685	36.675	27.574	97.634	2.098	18.172	2.955	1.321	12.488	6.183
	MixoUrea	77.086	22.262	16.539	43.779	8.697	20.685	3.772	1.497	20.797	7.048
	Photo.Ammonia	85.253	14.252	11.665	30.434	7.562	16.297	4.166	1.745	18.72	5.769
	Photo.Ammonia Diurnal	128.549	30.839	23.047	62.668	3.912	9.207	3.358	1.955	8.31	5.012
	Photo.Ammonia Early	65.414	11.516	8.698	26.593	12.246	13.49	4.771	1.306	14.739	4.571
	Photo.Ammonia MidLog	78.268	10.752	9.542	26.938	10.123	17.134	4.969	1.577	24.186	6.442
	Photo.HighLight Early	46.646	8.069	4.961	18.678	9.621	6.555	5.422	0.699	9.757	3.005
	Photo.HighLight MidLog	64.828	10.599	6.962	24.092	9.719	10.835	6.547	1.322	16.533	4.911
	Photo.Nitrate	60.662	13.052	10.468	28.083	5.588	11.345	2.909	0.908	14.369	4.336
	Photo.Nitrate Diurnal	121.535	31.5	22.855	64.219	2.482	10.051	2.557	1.309	10.034	5.304

	Photo.Urea	74.135	12.932	11.303	25.283	6.951	11.449	3.85	1.052	14.709	3.871
	Photo.Urea Diurnal	137.147	31.782	23.907	59.649	2.472	9.821	3.388	1.648	11.33	5.525
H2O2 Treatment	Hydrogen peroxide time course .5 hour (1)	172.93	98.996	27.508	94.594	25.777	43.433	39.828	12.648	57.681	19.178
	Hydrogen peroxide time course .5 hour (2)	152.205	86.592	21.743	91.347	25.001	42.179	33.081	12.767	53.365	17.777
	Hydrogen peroxide time course 0 hours (1)	180.35	109.114	28.183	102.184	15.158	42.508	19.701	11.25	37.75	11.949
	Hydrogen peroxide time course 0 hours (2)	151.619	88.359	20.282	86.593	17.608	37.996	18.068	11.942	39.761	14.257
	Hydrogen peroxide time course 1 hour (1)	145.075	79.585	26.705	97.707	40.526	49.563	44.757	17.45	86.94	27.503
	Hydrogen peroxide time course 1 hour (2)	156.095	79.742	26.228	115.46	41.949	49.7	45.559	16.901	88.986	30.402
N Concentration	WT-2137 Nitrogen deficiency first long time course 0 minutes (1)	215.485	75.241	38.374	90.471	18.629	34.143	22.489	14.479	37.815	14.686
	WT-2137 Nitrogen deficiency first long time course 0 minutes (2)	195.446	75.206	28.308	100.204	14.531	30.092	24.511	13.601	36.251	16.243
	WT-2137 Nitrogen deficiency first long time course 30 minutes (2)	140.952	46.995	14.497	95.011	35.391	25.034	32.197	11.571	50.561	19.616
	WT-2137 Nitrogen deficiency first long time course 30minutes (1)	144.702	50.205	12.516	87.548	37.562	20.489	28.429	11.861	60.698	23.126
	WT-2137 Nitrogen deficiency first long time course 4 hours (2)	65.528	16.568	2.782	19.979	17.436	16.71	15.901	6.649	26.163	12.407
	WT-2137 Nitrogen deficiency first long time course 4hours (1)	69.709	15.46	2.41	23.496	14.321	21.603	18.221	6.029	29.011	11.369
	WT-2137 Nitrogen deficiency first long time course 8 hours (1)	77.891	14.856	1.835	23.519	17.191	19.22	16.402	5.36	30.867	16.902
	WT-2137 Nitrogen deficiency first long time course 8 hours (2)	63.683	16.324	0.952	18.688	21.952	17.268	13.168	7.59	27.285	14.807
	WT-2137 Nitrogen deficiency second long time course 0 hours	154.661	67.132	22.087	94.388	8.838	30.684	16.574	10.347	37.273	14.261
	WT-2137 Nitrogen deficiency second long time course 12 hours	73.268	21.808	0.749	29.322	24.735	9.85	11.951	10.125	20.558	12.749
	WT-2137 Nitrogen deficiency second long time course 2 hours	105.32	34.905	9.104	39.067	12.33	11.148	14.591	7.985	23.692	10.259
	WT-2137 Nitrogen deficiency second long time course 24 hours	62.229	26.349	0.68	31.794	15.229	9.778	10.788	7.596	12.876	15.045
	WT-2137 Nitrogen deficiency second long time course 48 hours	52.986	18.016	0.617	33.827	21.957	8.611	5.168	4.606	12.11	14.529
	WT-2137 Nitrogen deficiency second long time course 8 hours	98.952	25.126	0.668	28.644	26.692	10.697	11.033	10.587	17.676	17.96
	WT-2137 Nitrogen deficiency short time course 0 minutes (1)	200.907	99.766	22.56	80.912	31.693	42.602	24.074	17.911	77.369	29.442
	WT-2137 Nitrogen deficiency short time course 0 minutes (2)	209.217	103.107	25.859	92.317	23.401	47.308	21.999	19.061	69.179	24.026
	WT-2137 Nitrogen deficiency short time course 12 minutes	192.558	91.368	19.478	105.04	46.877	32.546	34.577	20.706	100.957	30.272
	WT-2137 Nitrogen deficiency short time course 18 minutes	203.556	105.204	18.518	124.555	61.132	36.082	45.121	23.797	133.753	41.667

WT-2137 Nitrogen deficiency short time course 2 minutes	202.748	97.582	20.896	78.682	33.509	34.465	23.783	16.844	71.042	24.969
WT-2137 Nitrogen deficiency short time course 24 minutes	203.446	108.622	19.14	134.02	70.348	35.731	47.48	23.454	144.739	48.211
WT-2137 Nitrogen deficiency short time course 30 minutes	189.129	102.947	16.01	186.383	92.807	33.429	45.563	26.786	119.117	43.786
WT-2137 Nitrogen deficiency short time course 4 minutes	194.451	94.272	27.05	91.424	38.795	35.275	28.136	18.109	73.134	27.582
WT-2137 Nitrogen deficiency short time course 45 minutes	177.551	76.596	19.434	166.988	81.157	22.445	27.728	25.82	68.038	30.941
WT-2137 Nitrogen deficiency short time course 60 minutes	127.989	53.496	23.004	112.61	41.323	16.8	19.695	16.724	37.913	19.724
WT-2137 Nitrogen deficiency short time course 8 minutes	203.241	96.809	20.115	92.706	37.842	35.502	27.901	16.873	88.576	27.233

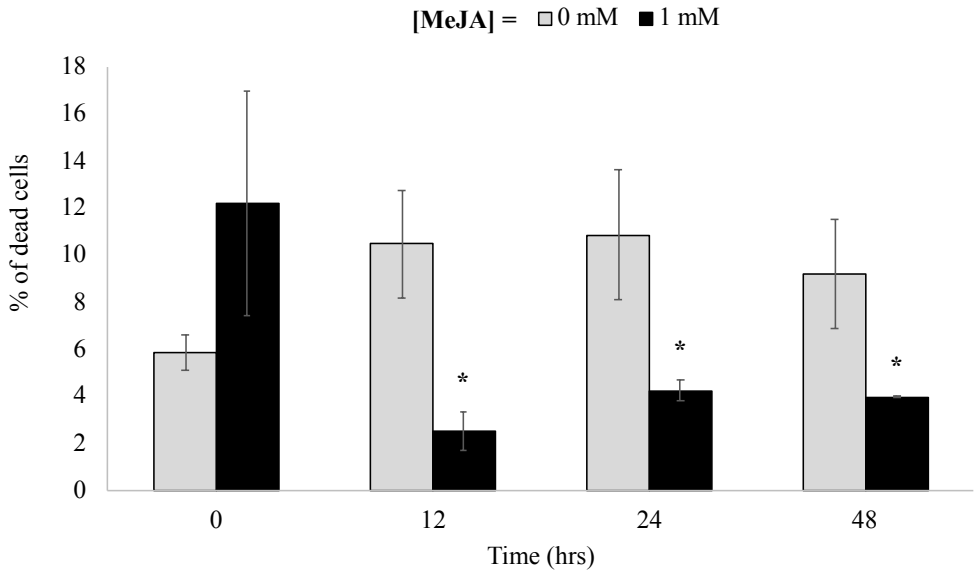

Figure A1. Percentage of dead cells in cultures of control (0 mM) and 1 mM MeJA treated cells. The initial 0 hour represents the time at which the cells were treated with MeJA. *C. reinhardtii* cells were stained with the LIVE/DEAD™ Fixable Violet Dead Cell Stain Kit (ThermoFisher) and then analysed by flow cytometry. Mean ± SEM is shown (n = 3) and unpaired *t*-test determine statistical significance between the control (0 mM) and the 1 mM treatment ($p < 0.05$ [*]).

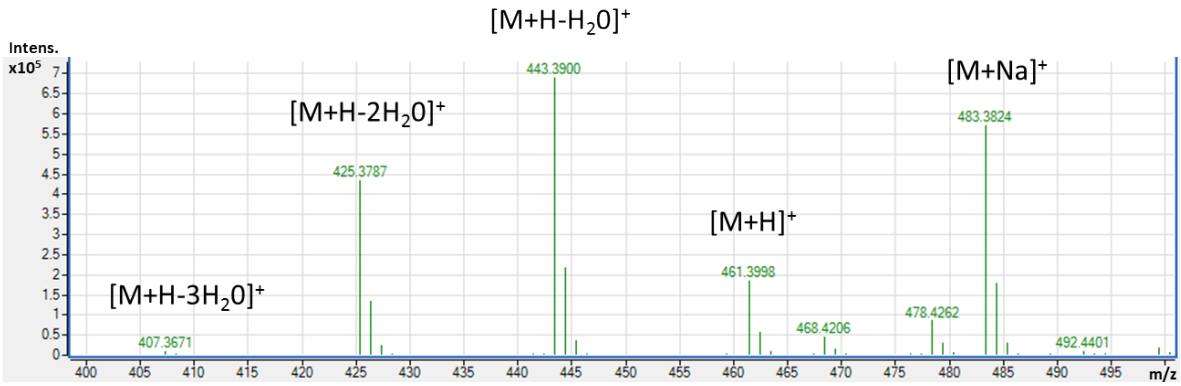

Figure A2. Mass spectrum of the $C_{30}H_{52}O_3$ molecules.

REFERENCES

[1] C.E. Vickers, J.B.Y.H. Behrendorff, M. Bongers, T.C.R. Brennan, M. Bruschi, L.K. Nielsen, Production of Industrially Relevant Isoprenoid Compounds in Engineered Microbes, in: B. Kamm (Ed.) Microorganisms in Biorefineries, Springer Berlin Heidelberg, Berlin, Heidelberg, 2015, pp. 303-334.

[2] C.E. Vickers, T.C. Williams, B. Peng, J. Cherry, Recent advances in synthetic biology for engineering isoprenoid production in yeast, Current opinion in chemical biology, 40 (2017) 47-56.

[3] R.C. Misra, P. Maiti, C.S. Chanotiya, K. Shanker, S. Ghosh, Methyl jasmonate-elicited transcriptional responses and pentacyclic triterpene biosynthesis in sweet basil, Plant Physiol, 164 (2014) 1028-1044.

[4] T. Moses, J. Pollier, J.M. Thevelein, A. Goossens, Bioengineering of plant (tri)terpenoids: from metabolic engineering of plants to synthetic biology in vivo and in vitro, The New phytologist, 200 (2013) 27-43.

[5] A.L. Meadows, K.M. Hawkins, Y. Tsegaye, E. Antipov, Y. Kim, L. Raetz, R.H. Dahl, A. Tai, T. Mahatdejkul-Meadows, L. Xu, L. Zhao, M.S. Dasika, A. Murarka, J. Lenihan, D. Eng, J.S. Leng, C.-L. Liu, J.W. Wenger, H. Jiang, L. Chao, P. Westfall, J. Lai, S. Ganesan, P. Jackson, R. Mans, D. Platt, C.D. Reeves, P.R. Saija, G. Wichmann, V.F. Holmes, K. Benjamin, P.W. Hill, T.S. Gardner, A.E. Tsong, Rewriting yeast central carbon metabolism for industrial isoprenoid production, Nature, 537 (2016) 694.

[6] N. Yan, C. Fan, Y. Chen, Z. Hu, The Potential for Microalgae as Bioreactors to Produce Pharmaceuticals, International journal of molecular sciences, 17 (2016) 962.

[7] F.K. Davies, R.E. Jinkerson, M.C. Posewitz, Toward a photosynthetic microbial platform for terpenoid engineering, Photosynthesis Research, 123 (2015) 265-284.

[8] C. Halfmann, L. Gu, W. Gibbons, R. Zhou, Genetically engineering cyanobacteria to convert CO(2), water, and light into the long-chain hydrocarbon farnesene, Applied microbiology and biotechnology, 98 (2014) 9869-9877.

[9] K.J. Lauersen, T. Baier, J. Wichmann, R. Wordenweber, J.H. Mussgnug, W. Hubner, T. Huser, O. Kruse, Efficient phototrophic production of a high-value sesquiterpenoid from the eukaryotic microalga Chlamydomonas reinhardtii, Metabolic engineering, 38 (2016) 331-343.

[10] S. D'Adamo, G. Schiano di Visconte, G. Lowe, J. Szaub-Newton, T. Beacham, A. Landels, M.J. Allen, A. Spicer, M. Matthijs, Engineering The Unicellular Alga Phaeodactylum tricornutum For High-Value Plant Triterpenoid Production, Plant biotechnology journal, In press (2018).

[11] M. Lohr, J. Schwender, J.E. Polle, Isoprenoid biosynthesis in eukaryotic phototrophs: a spotlight on algae, Plant science : an international journal of experimental plant biology, 185-186 (2012) 9-22.

[12] K.J. Lauersen, J. Wichmann, T. Baier, S.C. Kampranis, I. Pateraki, B.L. Møller, O. Kruse, Phototrophic production of heterologous diterpenoids and a hydroxy-functionalized derivative from Chlamydomonas reinhardtii, Metabolic engineering, 49 (2018) 116-127.

[13] J. Wichmann, T. Baier, E. Wentnagel, K.J. Lauersen, O. Kruse, Tailored carbon partitioning for phototrophic production of (E)-alpha-bisabolene from the green microalga Chlamydomonas reinhardtii, Metabolic engineering, 45 (2018) 211-222.

[14] K. Vavitsas, E.Ø. Rue, L.K. Stefánsdóttir, T. Gnanasekaran, A. Blennow, C. Crocoll, S. Gudmundsson, P.E. Jensen, Responses of Synechocystis sp. PCC 6803 to heterologous biosynthetic pathways, Microbial Cell Factories, 16 (2017) 140.

[15] L. Pauwels, K. Morreel, E. De Witte, F. Lammertyn, M. Van Montagu, W. Boerjan, D. Inze, A. Goossens, Mapping methyl jasmonate-mediated transcriptional reprogramming of metabolism and cell cycle progression in cultured Arabidopsis cells, Proceedings of the National Academy of Sciences of the United States of America, 105 (2008) 1380-1385.

[16] J.J. Cheong, Y.D. Choi, Methyl jasmonate as a vital substance in plants, Trends in genetics : TIG, 19 (2003) 409-413.

[17] H. Gundlach, M.J. Müller, T.M. Kutchan, M.H. Zenk, Jasmonic acid is a signal transducer in elicitor-induced plant cell cultures, Proceedings of the National Academy of Sciences, 89 (1992) 2389-2393.

[18] L. Pauwels, D. Inzé, A. Goossens, Jasmonate-inducible gene: what does it mean?, Trends in Plant Science, 14 (2009) 87-91.

[19] H. Suzuki, M.S.S. Reddy, M. Naoumkina, N. Aziz, G.D. May, D.V. Huhman, L.W. Sumner, J.W. Blount, P. Mendes, R.A. Dixon, Methyl jasmonate and yeast elicitor induce differential transcriptional and metabolic re-programming in cell suspension cultures of the model legume Medicago truncatula, Planta, 220 (2005) 696-707.

[20] J. Shi, C. Ma, D. Qi, H. Lv, T. Yang, Q. Peng, Z. Chen, Z. Lin, Transcriptional responses and flavor volatiles biosynthesis in methyl jasmonate-treated tea leaves, BMC Plant Biology, 15 (2015) 233.

[21] G. Sun, Y. Yang, F. Xie, J.F. Wen, J. Wu, I.W. Wilson, Q. Tang, H. Liu, D. Qiu, Deep sequencing reveals transcriptome re-programming of Taxus x media cells to the elicitation with methyl jasmonate, PLoS One, 8 (2013) e62865.

[22] V. Courdavault, M. Clastre, A.J. Simkin, N. Giglioli-Guivarc'h, Prenylated Proteins Are Required for Methyl-Jasmonate-Induced Monoterpenoid Indole Alkaloids Biosynthesis in Catharanthus roseus, in: T.J. Bach, M. Rohmer (Eds.) Isoprenoid Synthesis in Plants and Microorganisms: New Concepts and Experimental Approaches, Springer New York, New York, NY, 2013, pp. 285-296.

[23] D. Yang, P. Ma, X. Liang, Z. Wei, Z. Liang, Y. Liu, F. Liu, PEG and ABA trigger methyl jasmonate accumulation to induce the MEP pathway and increase tanshinone production in Salvia miltiorrhiza hairy roots, Physiologia plantarum, 146 (2012) 173-183.

[24] R.A. Patil, S.K. Lenka, J. Normanly, E.L. Walker, S.C. Roberts, Methyl jasmonate represses growth and affects cell cycle progression in cultured Taxus cells, Plant cell reports, 33 (2014) 1479-1492.

[25] J.-E. Lee, Y.U. Cho, K.H. Kim, D.Y. Lee, Distinctive metabolomic responses of Chlamydomonas reinhardtii to the chemical elicitation by methyl jasmonate and salicylic acid, Process Biochemistry, 51 (2016) 1147-1154.

[26] E.H. Harris, The Chlamydomonas Sourcebook (Second Edition), Vol. 1: Introduction to Chlamydomonas and Its Laboratory Use, 2nd Edition ed., Academic Press2009.

[27] J. Pollier, E. Vancaester, U. Kuzhiumparambil, C.E. Vickers, K. Vandepoele, A. Goossens, M. Fabris, A widespread alternative squalene epoxidase participates in eukaryote steroid biosynthesis, Nature Microbiology, 4 (2019) 226-233.

[28] A.B. Canelas, C. Ras, A. ten Pierick, J.C. van Dam, J.J. Heijnen, W.M. van Gulik, Leakage-free rapid quenching technique for yeast metabolomics, Metabolomics, 4 (2008) 226-239.

[29] L. Henneman, A.G. van Cruchten, S.W. Denis, M.W. Amolins, A.T. Placzek, R.A. Gibbs, W. Kulik, H.R. Waterham, Detection of nonsterol isoprenoids by HPLC-MS/MS, Analytical biochemistry, 383 (2008) 18-24.

[30] S.A. Bustin, V. Benes, J.A. Garson, J. Hellemans, J. Huggett, M. Kubista, R. Mueller, T. Nolan, M.W. Pfaffl, G.L. Shipley, J. Vandesompele, C.T. Wittwer, The MIQE guidelines: minimum information for publication of quantitative real-time PCR experiments, Clinical chemistry, 55 (2009) 611-622.

[31] B. Thornton, C. Basu, Real-time PCR (qPCR) primer design using free online software, Biochemistry and molecular biology education : a bimonthly publication of the International Union of Biochemistry and Molecular Biology, 39 (2011) 145-154.

[32] T. Zhao, W. Wang, X. Bai, Y. Qi, Gene silencing by artificial microRNAs in Chlamydomonas, The Plant journal : for cell and molecular biology, 58 (2009) 157-164.

[33] L. Whitney, G. Novi, P. Perata, E. Loreti, Distinct Mechanisms Regulating Gene Expression Coexist within the Fermentative Pathways in Chlamydomonas reinhardtii, The Scientific World Journal, 2012 (2012) 9.

[34] M. Pape, C. Lambertz, T. Happe, A. Hemschemeier, Differential Expression of the Chlamydomonas [FeFe]-Hydrogenase-Encoding HYDA1 Gene Is Regulated by the COPPER RESPONSE REGULATOR1, Plant Physiol., 159 (2012) 1700-1712.

[35] M. Kajikawa, S. Kinohira, A. Ando, M. Shimoyama, M. Kato, H. Fukuzawa, Accumulation of Squalene in a Microalga Chlamydomonas reinhardtii by Genetic Modification of Squalene Synthase and Squalene Epoxidase Genes, PLOS ONE, 10 (2015) e0120446.

[36] M. Pfaffl, A new mathematical model for relative quantification in real-time RT-PCR, Nucleic Acids Research, 29 (2001) 2002-2007.

[37] A. Radonić, S. Thulke, I.M. Mackay, O. Landt, W. Siegert, A. Nitsche, Guideline to reference gene selection for quantitative real-time PCR, Biochemical and Biophysical Research Communications, 313 (2004) 856-862.

[38] L. Pauwels, A. Goossens, The JAZ Proteins: A Crucial Interface in the Jasmonate Signaling Cascade, The Plant cell, 23 (2011) 3089.

[39] J. Mach, The Jasmonate Receptor: Protein Modeling and Photoaffinity Labeling Reveal That the CORONATINE INSENSITIVE1 Protein Binds Jasmonoyl-Isoleucine and Coronatine, The Plant cell, 21 (2009) 2192-2192.

[40] M.D. Petroski, R.J. Deshaies, Function and regulation of cullin-RING ubiquitin ligases, Nature reviews. Molecular cell biology, 6 (2005) 9-20.

[41] N.T. Thanh, H.N. Murthy, K.W. Yu, E.J. Hahn, K.Y. Paek, Methyl jasmonate elicitation enhanced synthesis of ginsenoside by cell suspension cultures of Panax ginseng in 5-l balloon type bubble bioreactors, Appl Microbiol Biotechnol, 67 (2005) 197-201.

[42] A. Swiatek, M. Lenjou, D. Van Bockstaele, D. Inze, H. Van Onckelen, Differential effect of jasmonic acid and abscisic acid on cell cycle progression in tobacco BY-2 cells, Plant Physiol, 128 (2002) 201-211.

[43] S. Jung, Effect of chlorophyll reduction in Arabidopsis thaliana by methyl jasmonate or norflurazon on antioxidant systems, Plant Physiology and Biochemistry, 42 (2004) 225-231.

[44] K.M. Nkembo, J.-B. Lee, T. Hayashi, Selective Enhancement of Scopadulcic Acid B Production in the Cultured Tissues of Scoparia dulcis by Methyl Jasmonate, Chemical and Pharmaceutical Bulletin, 53 (2005) 780-782.

[45] P. Kumari, C.R.K. Reddy, B. Jha, Methyl Jasmonate-Induced Lipidomic and Biochemical Alterations in the Intertidal Macroalga Gracilaria dura (Gracilariaceae, Rhodophyta), Plant and Cell Physiology, 56 (2015) 1877-1889.

[46] B.M. Lange, T. Rujan, W. Martin, R. Croteau, Isoprenoid biosynthesis: The evolution of two ancient and distinct pathways across genomes, Proceedings of the National Academy of Sciences of the United States of America, 97 (2000) 13172-13177.

[47] E. Cordoba, M. Salmi, P. Leon, Unravelling the regulatory mechanisms that modulate the MEP pathway in higher plants, J Exp Bot, 60 (2009) 2933-2943.

[48] E. Vranová, D. Coman, W. Gruissem, Network Analysis of the MVA and MEP Pathways for Isoprenoid Synthesis, Annual Review of Plant Biology, 64 (2013) 665-700.

[49] J.M. Estevez, A. Cantero, A. Reindl, S. Reichler, P. Leon, 1-Deoxy-D-xylulose-5-phosphate synthase, a limiting enzyme for plastidic isoprenoid biosynthesis in plants, The Journal of biological chemistry, 276 (2001) 22901-22909.

[50] E.M. Enfissi, P.D. Fraser, L.M. Lois, A. Boronat, W. Schuch, P.M. Bramley, Metabolic engineering of the mevalonate and non-mevalonate isopentenyl diphosphate-forming pathways for the production of health-promoting isoprenoids in tomato, Plant biotechnology journal, 3 (2005) 17-27.

[51] W.L. Morris, L.J. Ducreux, P. Hedden, S. Millam, M.A. Taylor, Overexpression of a bacterial 1-deoxy-D-xylulose 5-phosphate synthase gene in potato tubers perturbs the isoprenoid metabolic network: implications for the control of the tuber life cycle, J Exp Bot, 57 (2006) 3007-3018.

[52] A. Banerjee, T.D. Sharkey, Methylerythritol 4-phosphate (MEP) pathway metabolic regulation, Natural Product Reports, 31 (2014) 1043-1055.

[53] Y. Xiao, T. Savchenko, E.E. Baidoo, W.E. Chehab, D.M. Hayden, V. Tolstikov, J.A. Corwin, D.J. Kliebenstein, J.D. Keasling, K. Dehesh, Retrograde signaling by the plastidial

metabolite MEcPP regulates expression of nuclear stress-response genes, Cell, 149 (2012) 1525-1535.

[54] M. Rodriguez-Concepcion, A. Boronat, Elucidation of the methylerythritol phosphate pathway for isoprenoid biosynthesis in bacteria and plastids. A metabolic milestone achieved through genomics, Plant Physiol, 130 (2002) 1079-1089.

[55] G.M. Estavillo, K.X. Chan, S.Y. Phua, B.J. Pogson, Reconsidering the nature and mode of action of metabolite retrograde signals from the chloroplast, Frontiers in plant science, 3 (2012) 300.

[56] K. Zhou, R. Zou, G. Stephanopoulos, H.P. Too, Metabolite profiling identified methylerythritol cyclodiphosphate efflux as a limiting step in microbial isoprenoid production, PLoS One, 7 (2012) e47513.

[57] K.M. Brumfield, S.M. Laborde, J.V. Moroney, A model for the ergosterol biosynthetic pathway in Chlamydomonas reinhardtii, European Journal of Phycology, 52 (2017) 64-74.

[58] J.Y. Han, J.G. In, Y.S. Kwon, Y.E. Choi, Regulation of ginsenoside and phytosterol biosynthesis by RNA interferences of squalene epoxidase gene in Panax ginseng, Phytochemistry, 71 (2010) 36-46.

[59] H. Suzuki, L. Achnine, R. Xu, S.P. Matsuda, R.A. Dixon, A genomics approach to the early stages of triterpene saponin biosynthesis in Medicago truncatula, The Plant journal : for cell and molecular biology, 32 (2002) 1033-1048.

[60] J.Y. Han, H.J. Kim, Y.S. Kwon, Y.E. Choi, The Cyt P450 enzyme CYP716A47 catalyzes the formation of protopanaxadiol from dammarenediol-II during ginsenoside biosynthesis in Panax ginseng, Plant & cell physiology, 52 (2011) 2062-2073.

[61] J.Y. Oh, Y.-J. Kim, M.-G. Jang, S.C. Joo, W.-S. Kwon, S.-Y. Kim, S.-K. Jung, D.-C. Yang, Investigation of ginsenosides in different tissues after elicitor treatment in Panax ginseng, Journal of Ginseng Research, 38 (2014) 270-277.

[62] S. Mangas, M. Bonfill, L. Osuna, E. Moyano, J. Tortoriello, R.M. Cusido, M.T. Pinol, J. Palazon, The effect of methyl jasmonate on triterpene and sterol metabolisms of Centella asiatica, Ruscus aculeatus and Galphimia glauca cultured plants, Phytochemistry, 67 (2006) 2041-2049.

[63] O.-T. Kim, M.-Y. Kim, S.-J. Hwang, J.-C. Ahn, B. Hwang, Cloning and molecular analysis of cDNA encoding cycloartenol synthase fromCentella asiatica (L.) urban, Biotechnology and Bioprocess Engineering, 10 (2005) 16.